Aus der Neurologischen Universitätsklinik Tübingen
Abteilung Neurologie mit Schwerpunkt neurovaskuläre Erkrankungen

Influence of perampanel, dextromethorphan and nimodipine on resting, induced and evoked oscillatory brain activity

Inaugural- Dissertation
zur Erlangung des Doktorgrades der Medizin

der medizinischen Fakultät der Eberhard-Karls-Universität zu Tübingen

Vorgelegt von

Liang, Chen

2021

Dekan:	Prof. Dr. B. Pichler
1. Berichterstatter:	Prof. Dr. U. Ziemann
2. Berichterstatter:	Prof. Dr. M. Schwab

Tag der Disputation: 21.10.2021

Meiner Familie gewidmet

Content

List of figures and tables

Figures

Tables

List of abbreviation

AMPA(R)	α-amino-3-hydroxy-5-methyl-4-isoxazole propionic acid type (receptor)
AMT	Active motor threshold
APB	Abductor pollicis brevis muscle
CNS	Central nervous system
EEG	Electroencephalography
EPSP	Excitatory postsynaptic potential
EPSC	Excitatory postsynaptic current
EMG	Electromyography
FOI	Frequency of interest
GABA(R)	Gamma-aminobutyric acid(-receptor)
ICA	Independent component analysis
ISP	TMS-evoked interhemispheric propagation
IPSP	Inhibitory postsynaptic potential
MEP	Motor evoked potential
MEG	Magnetoencephalography
(f)MRI	(functional) Magnetic Resonance Imaging
MSO	Maximum stimulator output
NMDA(R)	N-methyl-D-aspartate type (receptor)
PET	Positron emission tomography
RMT	Resting motor threshold
s.d.	Standard deviation
TEP	TMS-evoked EEG potential
TFR	Time-frequency representation
TMS	transcranial magnetic stimulation
TMS-EEG	simultaneous EEG registration during TMS

T_{max}	Time to reach maximum plasma concentration
TOI	Time-frequency region of interest
VGCC	voltage-gated calcium channel

1 Introduction

Cortical excitability is an important diagnostic substrate of pathophysiologic sources of diseases like epilepsy, migraine and traumatic brain injury (Xiang et al. 2016, Pawley et al. 2017, Verley et al. 2018). So far, despite the considerable progress that has recently been made in neurophysiological research, the mechanisms underlying cortical excitability remain incompletely understood. One core issue is how to properly assess the correlation between synaptic transmissions on the molecular level, such as glutamatergic and GABA-ergic transmissions, and long-range neurophysiological interactions, including intra- and interhemispheric, and cortico-spinal connectivity (Daskalakis et al. 2012). Combining pharmacological interventions (Ziemann et al. 2015) with neuroimaging techniques, such as EEG or TMS-EEG, MRI, fMRI, PET and MEG (Ziemann 2011, Klamer et al. 2015, Cichy and Pantazis 2017), provides a promising way to approach such an issue by visualizing information of normal and abnormal neuro-activities (Chung et al. 2015). In these combinations, Pharmaco-TMS-EEG has been proved to be a reliable non-invasive method to modulate, stimulate and monitor neuronal excitability in real-time, respectively. Since EEG signals are affected directly or indirectly not only by each TMS stimulation, but also by pharmacological modulation, it is crucial to identify and relate EEG-responses in coupled neurophysiological system. The perturbation provoked TMS-on EEG signals can “either be evoked (i.e. phase-locked) or induced (i.e. non-phased locked)” oscillatory responses (Herrmann et al. 2014, Premoli et al. 2014, Pellicciari et al. 2017). The TMS-evoked potentials (TEPs) after various pharmacological interventions (Premoli et al. 2014, Darmani et al. 2016, Salavati et al. 2018b, Rogasch et al. 2020), and TMS-induced oscillation under influence of agonists of GABA (Premoli et al. 2017), which is the main transmitter of the cortical inhibitory system, have been well developed and defined in recent years (Tremblay et al. 2019). It seems that synchronous oscillatory features of TMS-EEG after glutamatergic modulation, which is the major form of excitatory transmission, has still been less investigated in-vivo. At synaptic level of an excitatory transmission, it is important to acknowledge two principal mechanisms of neuronal depolarization. One is mediated by transmitter

towards postsynaptic receptors, such as glutamatergic AMPA- and NMDA-receptors, the other is voltage-controlled, such as voltage-gated-calcium-channels (VGCC). From this perspective, this study aims to investigate the effect of perampanel and dextromethorphan as glutamate-antagonists and nimodipine as VGCC-antagonist on the feedback of time and frequency of TMS-EEG.

1.1 Transcranial magnetic stimulation (TMS)

TMS is a technique to investigate cortical excitation and inhibition non-invasively. Historically, TMS has been developed in two stages, from invasive to non-invasive brain stimulation and from uncontrolled ubiquitous brain stimulation to reliable focal stimulation. Gustav Fritsch and Eduard Hitzig in 1870 (Carlson and Devinsky 2009) firstly described electrical excitability of human cortex using an invasive method, by which stimulating a specific cortical area could lead to motoric reaction. This area was then identified as the primary motor cortex (M1). At the second stage, electrical induction by magnetism was suggested as an improved approach by A. d'Arsonval in 1896, where stimulation by a magnetic full-body oscillator could cause symptoms like dizziness and unspecified muscle contractions on subjects (Geddes 1991). But this phenomenon could not be clearly explained and measured. About 70 years later, R.G. Bickford and B.D. Freeming developed the first working single-pulsed transcranial stimulator, which could stimulate visually detectable muscle activity. Yet, it could still not be used to measure such activity due to high artifacts, that probably resulted from magnetic field reverberations (Chapter 1.2.2, Siebner and Ziemann 2007). M. Polson (Polson et al. 1982), A. Barker (Head of Department of Medical Physics and Clinical Engineering, Sheffield University U.K.), R. Jalinous and I.L.Freeston (Barker et al. 1985) developed the first single-pulsed transcranial magnetic stimulator without such reverberations and provided measurable muscle potential as evidence for peripheral neuronal stimulation through a cortico-spinal pathway. To understand the basic principles behind TMS, it is important to introduce Faraday's law of electric induction by magnetism. Using a battery, a galvanometer, a metal ring and two wired loops, he observed that a changing magnetic field has been generated, when an in-constant primary current arrived

in the first wired loop. This magnetic field induced an electrical current in the second wired loop, but in the opposite direction to the current direction of the first loop. In line with Faraday's experiment, the basic design of a TMS device is relatively simple and consists of two universal components besides the power supply: a capacitor and an inductor coil. Charging and unloading the capacitor creates an alternating current, which drives through an inductor coil, while the electric current is filtered by a switch called "thyristor", a silicon-controlled rectifier as shown in Fig.1.

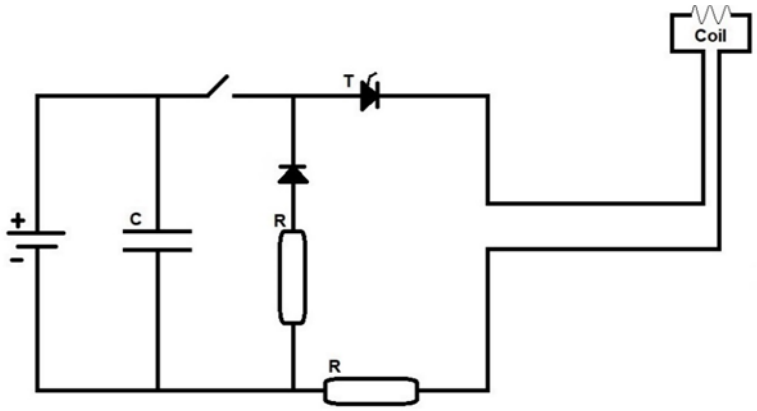

Figure 1. Simplified TMS-Circuit of a monophasic stimulator. C: capacitor; T: thyristor; R: resistance

Adding a diode parallel connected to the thyristor enables electric backflow which creates a resonance of loaded voltage of the coil. This kind of resonance can generate a bipolar magnetic field by Faraday's law - whenever the capacitor conduits the electric energy and whenever the energy has been expired inside a single circulation. Such a changing magnetic field on human brain quickly induces biphasic electrical current inside circulating neurons, which serve as the second wire loop of Faradays experiment (Chapter 2.1, Siebner and Ziemann 2007). Disregarding electric resistance of human skin and scalp for electrical conduction, the circuit cannot be interrupted. Removing the first diode from the circuit and adding a diode resistance attenuates the biphasic signal to a monophasic signal. Such monophasic signal can be used to produce complex pulse waveforms and it also has a lower risk of an "explosive destruction of any circuit elements that

stood in the way caused by a large negative value due to a rapid drop in current" (Chapter 1, Epstein et al. 2012).

The changing magnetic field $\vec{B}$ can be calculated by the law of Biot and Savart (Madsen et al. 2015),

$$\vec{B} = \frac{\mu_0}{4\pi} \cdot \int \frac{J(\overrightarrow{r'}) \times (\vec{r} - \overrightarrow{r'})}{\left|\vec{r} - \overrightarrow{r'}\right|^3} \cdot d^3\overrightarrow{r'}$$

where r and r' represent spatial position vectors, J denotes the current distribution and μ_0 is vacuum permeability.

The value of the magnetic fields stands in negative correlation to the distance of stimulation (Kammer et al. 2001, Hallett 2007) and its induced electrical voltage $\vec{E}$ can be calculated by Faradays law as a vector of the changing magnetic field in relation to time after stimulation t, where $\vec{\nabla} \times$ represents the curl operator.

$$\vec{\nabla} \times \vec{E} = -\frac{\mathrm{d}\vec{B}}{\mathrm{d}t}$$

As figure-of-eight coils can induce a more focal magnetic field than conventional single-circular coils (Deng et al. 2014), the generated magnetic field of a figure-of-eight coil can also be calculated by computing models (Petrov et al. 2017). Using the admittance method by neuro-navigation-assisted technologies (Paffi et al. 2015), such induced electric field can be evaluated in real-time to improve targeting and dosing of neuronal stimulation.

Electric stimulation of neuronal tissue has been found to be useful in various ways. For instance, methods like transcranial direct current stimulation, deep brain stimulation and electroconvulsive therapy are only few of many established clinical treatments. In regards of transcranial magnetic stimulation, the advantage of such non-invasive method is that no electric current has been directly applied on the surface of the scalp, while the magnetic field itself has no biological consequences (Chapter 1.1, Krieg 2017). Also, adverse events related to transcranial magnetic stimulation appears to be relatively low on single pulses, but repetitive stimulations could give rise to seizure, burning from scalp electrodes, pain and headache, transient effects on hormones and change of

mood and cognition caused by long-term potentiation or depression (Wassermann 1998).

In the clinical diagnostics, TMS has been validated not only as a valuable tool for Alzheimer's disease (Ferreri et al. 2016), epilepsy (Valentin et al. 2008, Shafi et al. 2015), attention-deficit hyperactivity disorder (Dutra et al. 2016), and schizophrenia (Radhu et al. 2012, Rogasch et al. 2013), but also as therapeutic tool for major depressive disorder and migraine (approvals by U.S. Food and Drug Administration in 2008 and 2013). Evoked EEG-potentials can also be quantified by applying TMS to patients with early relapsing-remitting multiple sclerosis, although the most common amplitudes were mostly indifferent between early-stage RRMS and healthy controls except for N280 amplitudes (Zipser et al. 2018)

1.2 Electroencephalography (EEG)

Electroencephalography (EEG) is a real-time monitoring method to record electrophysiological activity of the brain. First recordings of spontaneous electrical activities were done by Richard Caton (Caton 1875) on animal brains. Hans Berger, who also discovered Alpha-waves (Berger 1929), then established fundamentals for the introduction of EEG in 1924. Since detection of epileptiform spikes by Gibbs, Davis and Lennox (Gibbs et al. 1935) and description of REM-sleep (Aserinsky and Kleitman 1953), EEG has been used as a tool for research, diagnostics in neurology and neuro-psychiatry, and for monitoring of patients in anesthesia or in sleep, e.g. at intensive care units or stroke (Jordan 1999).

A basic EEG system consists of electrodes, amplifiers and a digitizer, and records potential-differences between two electrodes on the scalp, of which the frontocentral electrode (FCz) is designed as reference electrode in most cases (Seeck et al. 2017). Such potential-difference is formed by an electric field of synchronized depolarization of focal underlying neuronal populations and reveal temporal and spatial information of postsynaptic potentials (Farzan et al. 2016). Even though the detection of sources is usually limited to a few centimeters below the cortical envelope of the human brain (Ilmoniemi et al. 1997, Taylor et al. 2008), the resolution of the EEG inverse problem allows to display the source of such

generated potential differences, as apical dendrites of pyramidal neurons can be mostly localized in the superficial layers of the cortex. When induced or spontaneous depolarization reaches the cortices, voltage-gated ion channels open for an influx of positive ions, which result in excitatory postsynaptic potentials (EPSPs). Due to the loss of the positive ions, the extracellular space become negatively polarized. The EPSPs inside the apical dendrites of pyramidal neurons can summarize to action potentials, which facilitate propagation of depolarization towards peripheral dendrites of neurons, which spread in the distant nerves and muscles. Such neurons can be modeled as dipoles due to a fast transmission of the action potentials. If the direction of such dipoles points towards deeper brain areas, the superficial areas are usually negatively polarized, whereas tangentially orientated dipoles are less likely to create any EEG potentials. A summarization of synchronized action potentials generates high potential differences and synchronous EEG-amplitudes within the same frequency, whereas asynchronous amplitudes are more likely to create higher frequencies (Chapter 10a, Gordon 2003).

Induced brain activity relates to different brain processes and is classified into specific waveforms, which frequency band widths are determined mainly by their stimulation source. Sudden sensory stimuli (Engel and Singer 2001), memorized processing (Chrobak and Buzsáki 1998) and actions (Muthukumaraswamy 2010) are usually followed by gamma-waves with frequencies of 31-80 Hz, reflecting fast inhibitory activities of interneurons (Johnson et al. 2017). In an active mental state with open eyes, the human brain mostly produces beta-waves with a frequency of 13-30 Hz. Alpha waves with a frequency of 8-12 Hz can be predominately found when subjects have their eyes closed in a relaxed and drowsy mode. A so-called alpha blockade can occur with mental activity like sudden opening of eyes (Kirschfeld 2009), and is involved in cognitive inhibitory processes (Weisz et al. 2011). Other slower waveforms like theta-waves with 4-7 Hz or delta-waves at 1-3 Hz are related to emotions like displeasure and pleasure (Knyazev 2012) or abnormal brain behaviors and REM-sleep (Hutchison and Rathore 2015). In this study, all subjects were in a relaxed

position with eyes open, thus the focus of this work will be on alpha- and beta-frequency bands.

1.3 Combination of tools: pharmaco-TMS-EEG

The implementation of TMS into EEG-recordings was firstly suggested in 1989 (Cracco et al. 1989). Cracco investigated the EEG-responses in the contralateral hemisphere caused by TMS-stimulation about 20 ms earlier. Thus, TMS-EEG enables a real-time and non-invasive mapping and tracing of neuronal reactions of human cortex in contrast to other imaging approaches (Ilmoniemi et al. 1997). Furthermore, a “spreading of neuronal activation from motor to premotor to contralateral and then to parietal areas” has been observed (Ilmoniemi et al. 1997) and thus indicating cortico-cortical and cortical-spinal transmissions. Several further studies showed the relationship between TMS and inhibitory EEG responses within a longer post-stimulus interval (up to 200 ms) by applying paired stimulation protocols, such as short- or long-interval cortical inhibition (SICI and LICI) (Nakamura et al. 1997). Recent studies considered a time period of more than 300ms of EEG responses after the TMS pulse (Hill et al. 2016).

TMS depolarizes cortical neurons depending on the coil-orientation and intensity of the TMS-induced current inside the cortex. In particular, on primary motor cortex, induced activity of excitatory pyramidal cells and inhibitory interneurons of layer II, III and V can account for corticospinal plasticity (Di Lazzaro and Ziemann 2013). The excitation is transmitted to the target muscle through the corticospinal tract and peripheral nerves and may be quantified as motor evoked potential (MEP) as recorded in electromyography (EMG) (Barker et al. 1985, Ilmoniemi et al. 1997, Daskalakis et al. 2012, Groppa et al. 2012). Due to its quantifiability and reproducibility, EEG-responses during such activations can be therefore determined as TEPs (Komssi et al. 2004, Ilmoniemi and Kičić 2009) and reveal direct and indirect information of cortical excitability (Daskalakis et al. 2002).

It has been suggested that such responses originate in interactions from evoked EPSPs of pyramidal neurons and inhibitory postsynaptic potentials (IPSPs) of interneurons (Kirschstein and Köhling 2009, Hill et al. 2016), especially in a post-

stimulation period within 200ms in animal models and in-vitro studies (Rotenberg et al. 2008, Mueller et al. 2014). These EEG potentials appear in a certain pattern of latencies and time-locked amplitudes after single-pulse TMS-stimulations on the primary motor cortex (see Fig. 2) and show reproducible corresponding topographies (Komssi and Kähkönen 2006, Ilmoniemi and Kičić 2009, Hill et al. 2016).

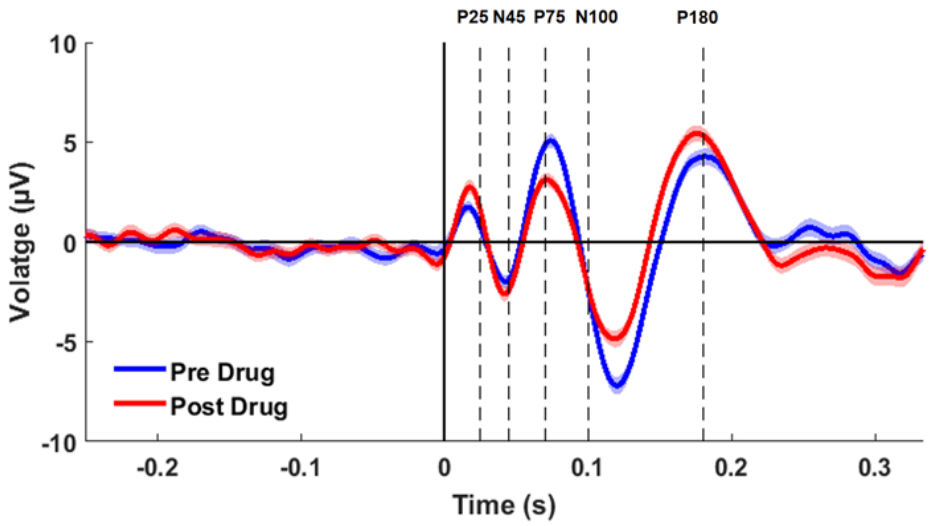

Figure 2. Sample averaged data of TMS-evoked EEG-responses
of a representative participant before (blue) and (after) drug intervention and after data cleaning process.
Data were obtained with a 62 channels EEG device. Vertical line at 0s displays the TMS pulse, dotted lines present most frequent amplitudes named as P (positive) or N (negative) and Number shows the most frequent peaks in relation to the time after stimulus on-set: P25, N45, P75, N100, P180.

To obtain such potentials, a validated data cleaning method is necessary. Although mechanical and electronical artifacts can be partially reduced by using direct-current (Tsai et al. 2018) -coupled amplifiers (Daskalakis et al. 2012) and TMS-compatible EEG electrodes (Veniero et al. 2009), the obtained raw data still need to be filtered for a good “signal-to-noise ratio” (Ilmoniemi and Kičić 2009). Fortunately, many artifacts have been so far assigned to different waveforms and topographies. They relate to the TMS pulse (Ilmoniemi et al. 1997), different electrode-skin charges (Veniero et al. 2009), power supply, other electronics

(Ilmoniemi and Kičić 2009, Rogasch and Fitzgerald 2013, Farzan et al. 2016), muscle artifacts and coil pressure on the scalp, respectively. In the data analysis pipeline, in order to sort out event-evoked potentials from artifacts and spontaneous cerebral activity, one averages the EEG signal time-locked to the TMS-trigger (Herrmann et al. 2004). However, an issue related to this approach is that relevant event-related EEG information, which varies in time and phase with respect to the stimulus on-set, can be cancelled out (Herrmann et al. 2014). Such time- and phase-variabilities represent the features of TMS-induced brain oscillations. As a matter of course, if TMS had only the effect of a phase-reset and entrainment of underlying brain oscillations (Thut et al. 2011), this issue could be considered negligible. However, TMS-locked oscillatory activity has been indicated to origin from the same neurophysiological generator like spontaneous oscillations (Herring et al. 2015), e.g. alpha-oscillations, which is predominant in occipital areas in an eyes closed state, can also be evoked after stimulation of the occipital cortex (Rosanova et al. 2009). Thus, a proper extraction and interpretation of induced oscillations can pose a challenge. For this purpose, various analysis methods were developed (Farzan et al. 2016, Tremblay et al. 2019). Of those, time-frequency representation (TFR) is a particularly promising method to characterize the spectral properties of TMS-induced EEG responses (Herrmann et al. 2014, Pellicciari et al. 2017, Premoli et al. 2017). Especially limiting the scope into frequency bands not only has the advantage of focusing into relevant frequencies of interest, but also can considerably reduce artifacts (Herrmann et al. 2014).

Although spectral TMS-EEG properties attracted an increasing interest in the last decade, TMS-induced oscillations on the motor cortex remained less investigated. Recent works revealed predominately variations of TFR-power in TMS-induced-oscillations of non-motor regions of the cortex within alpha- (Fuggetta et al. 2005, Rosanova et al. 2009, Herring et al. 2015), beta- (Paus et al. 2001, Rosanova et al. 2009) and gamma-bands (Canali et al. 2017), and provide information about intra- and interhemispheric connections as results of a spatiotemporal spreading (Lee et al. 2003, Ferreri et al. 2011).

Apart from single-pulse TMS, there are other variations in intensities and stimulation forms, e.g. repetitive TMS stimulation (Esser et al. 2006, Casula et al. 2014), theta-burst stimulation (Casula et al. 2014, Chung et al. 2016) and paired associative stimulation (Weise et al. 2017, Salavati et al. 2018a), supporting the increasing interest in combined techniques using TMS and EEG. Paired-pulse TMS protocols, e.g. in the protocols of SICI (Paus et al. 2001) and LICI (Daskalakis et al. 2008, Rogasch et al. 2015) are shown to be able to suppress neuronal activity with a interstimulus interval between 50 and 200ms, enabling a mechanical method to study cortical inhibition. A different approach to modulate the human cortical systems is to implement pharmacological applications to single pulse TMS-EEG. This approach appear to be a more specific way to study the excitatory and inhibitory systems differentially (Barr et al. 2013). On the one hand, earlier pharmaco-TMS-EEG studies have shown significant changes of evoked cortical responses corresponding to subunit-agonists of gamma-aminobutyric acid (GABA) receptors, when applying paired-pulsed cortical inhibition protocols like SICI and LICI (Premoli et al. 2014, Premoli et al. 2018). On the other hand, a modulation of alpha- and beta-frequency of TMS-induced brain oscillations with the same applied drugs has also been demonstrated (Premoli et al. 2017), which contributes to the understanding of the inhibitory GABA-ergic system. For the excitatory system, an early pharmaco-TMS-EEG-study demonstrated a decreased motor cortical excitability by antagonizing a specific sort of glutamatergic receptors, the N-methyl-D-aspartate receptor (NMDAR), also by using paired-pulse TMS protocols like intracortical facilitation (ICF) and intracortical inhibition (ICI) (Ziemann et al. 1998). The same antagonist - dextromethorphan has the potential to decrease long-term potentiation (Salavati et al. 2018a), which is important in the process of memory and learning (Collingridge and Bliss 1995).

1.4 Glutamatergic receptors

It is well known that information is interneuronally transmitted by chemical substances, such as glutamate, GABA, glycine etc. Among these, glutamate represent the “brain’s most abundant neurotransmitter” (Pinky et al. 2018). Yet, the neurophysiological and neurochemical mechanisms of glutamatergic transmission and metabolism have not been fully revealed. Generally, according to the different transduction mechanisms, glutamatergic receptors are divided into two families: ionotropic ligand-gated channel receptors and metabotropic ones. Techniques like immunoelectron microscopy, especially immunogold labeling (Nusser et al. 1994), displayed that the majority of receptors in postsynaptic membranes with affinity to glutamate are considered ionotropic (Asztély and Gustafsson 1996), whereas the metabotropic glutamate receptors, which activate a second messenger system by coupling GTP-binding proteins (Conn 2003), seem to occur with high concentrations in the in the peri-synaptic annulus (Baude et al. 1993), see Fig. 3. As a result of the different transduction mechanisms, different speed of signal transmissions can be observed. In general,

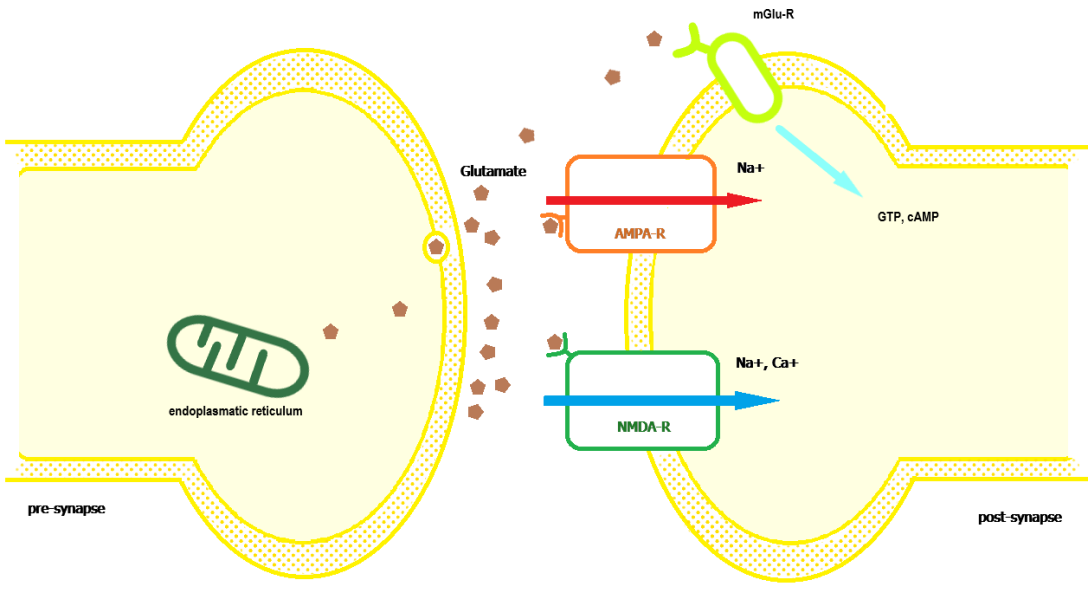

Figure 3. Schematic view of a synapse for glutamate transmission.
Containing ionotropic receptors AMPA-R and NMDA-R and metabotropic receptors (mGlu-R), which appear in the periphery of a post-synapse, especially in the area of a peri-synaptic annulus.

ionotropic transmissions are faster than metabotropic (Reiner and Levitz 2018) in causing EPSPs, probably due to the direct influx of positively charged ions like sodium, potassium, and calcium. In this study, we focus on cerebral modulation of ionotropic glutamatergic transmissions.

Referring to NMDA as a synthetic agonist (Ishii et al. 1993), the ionotropic receptors are categorized as NMDARs and Non-NMDA-related receptors, which include alpha-amino-3-hydroxy-5-methyl-4-isoxazole propionate (AMPA)-receptors, kainate receptors and delta receptors due to their selective affinity for specific substances. Generally, the molecular structure of ionotropic receptors can be simplified as a glycoprotein consisting of a non-functional amino terminal domain, a transmembrane domain and a ligand binding domain whose composition can vary due to several subunits, as shown in Fig. 4 (Sobolevsky et al. 2009, Furukawa 2012).

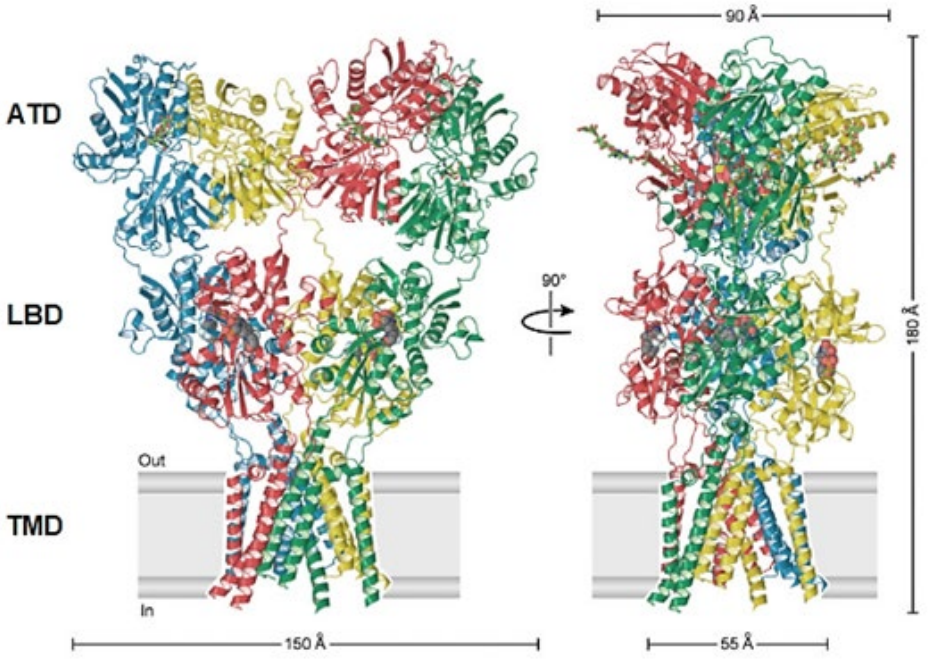

Figure 4. Model of an ionotropic glutamate receptor.
Here: GluA2-AMPA-receptor from two sides in different 90 degree views, the receptor is divided into 3 domains: amino terminal domain (ATD), ligand-binding domain (LBD) and transmembrane domain (TMD) with a carboxyl ending, Out: synapse side, In: cell side, Å: angstrom =100 pm (modified from: Sobolevsky AI, Rosconi MP, Gouaux E (2009) X-ray structure, symmetry and mechanism of an AMPA-subtype glutamate, Nature 462). With permission.

Three gene-coded NMDA receptor-subunit families (GluN1-3) (Vyklicky et al. 2014) containing seven subunit types (GluN1, GluN2A-D, GluN3A-B) have been revealed (Chapter 17, Brady et al. 2011). However, the distribution of NMDAR with a specific type of subunit are more locally limited inside human brain cells: GluN2A and -B in the forebrain and GluN2A and -C in the cerebellum, GluN2D in the midbrain and hindbrain, GluN3A in the spinal cord and cortex, and GluN3B mainly in motoneurons in spinal cord, pons and medulla (Chapter 17, Brady et al. 2011, Dzamba et al. 2013). On the molecular level, glutamate and glycine are needed to activate NMDA receptors with GluN1 and/or GluN2 subunits (Clements and Westbrook 1991), whereas “NMDA-receptors composed of GluN1/ GluN3 only require glycine for activation” (Chatterton et al. 2002, Pachernegg et al. 2012). When the ligands bind on the corresponding domain, the transmembrane domains open like channels for influx of sodium and calcium, which create an EPSP through summation (Mayer et al. 1987).

Regarding non-NMDA subunits, four mRNA-coded AMPA receptor subunits (GluR1-4) have been identified as main representatives out of the non-NMDA-related receptors. Receptors with GluR1-3 subunits are expressed in the majority of neurons inside the CNS, while GluR4 is more expressed in cerebellum and auditory system outside of the excitatory pyramidal neurons (Schwenk et al. 2014, Pelkey et al. 2015) and GluR3-AMPARs have been observed to play a role in hippocampal and cerebellar long-term potentiation (Gutierrez-Castellanos et al. 2017, Renner et al. 2017). GluR1 has been also related to the major form, which leads to NMDAR-dependent long-term-potentiation (Huganir and Nicoll 2013, Herring and Nicoll 2016). The neuronal permeability of calcium has been related to the presence of GluR2-lacking AMPARs (Burnashev et al. 1992), which are merely expressed in neuronal synapses during postnatal period, and low in the mature synaptic levels (Diering and Huganir 2018). In mature brains, GluR2-lacking AMPARs were only expressed inside “interneurons and some cortical neurons” (Rogawski 2011). In contrast, AMPARs containing the GluR2-subunit are significantly less permeable to calcium ions (Vandenberghe et al. 2000, Rogawski 2011) and prevalent in most principal neurons throughout the telencephalon (Jonas et al. 1994, Petralia et al. 1997), which includes the motor

cortex. An activation of such AMPARs results in a large influx of only sodium ions, which explains the faster kinetics of AMPAR than other glutamatergic receptors. An uprising time towards activation peak within 2,5ms and a desensitizing within 4,4ms has been described (Clements et al. 1998), whereas NMDA-related activations result in a decaying or slow-uprising postsynaptic EPSP with a peak at 15-40ms (Sutor and Hablitz 1989, Lester et al. 1990) and has a prolonged component as glutamate remains bound to NMDARs (Lester et al. 1990).

In the human cortex, a coexistence of the NMDAR and non-NMDAR driven mechanisms provides for spreading neuronal excitation. Such coexistence results in a combined EPSP with two currents (Fig. 5). EPSPs can sum up spatially and temporally to influence the frequency of action potentials.

Unlike the other ionotropic glutamate receptors, kainate receptors have been found at both pre- and postsynaptic membranes (Contractor et al. 2011) and play a yet unclear role in excitatory synaptic transmission and network modulation. Delta receptors are also described as ionotropic glutamatergic receptors (Traynelis et al. 2010), but their importance for brain metabolism is largely inferior to AMPAR and NDMAR, which are at the core of the current study.

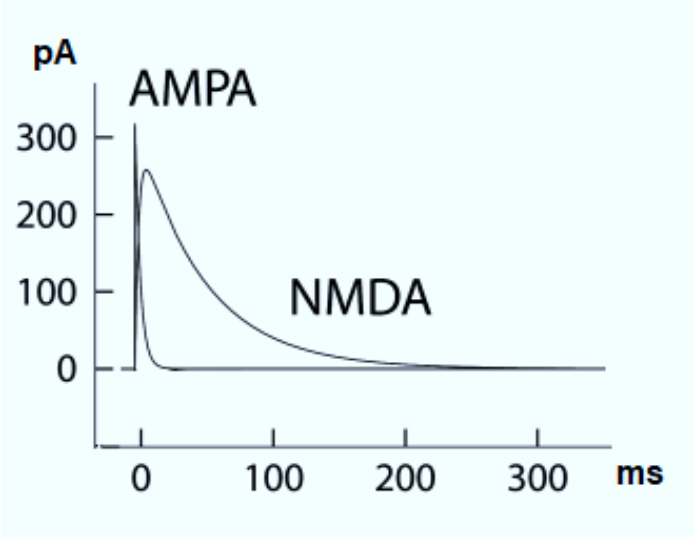

Figure 5. A general excitatory postsynaptic activation with AMPA- and NMDA-receptor components. X-axis: time in milliseconds, and y-axis: electric current in picoampere,
Modified from: Neuronal Dynamics, From single neurons to networks and models of cognition by Wulfram Gerstner, Werner M. Kistler, Richard Naud and Liam Paninski, Cambridge University Press July 2014 ISBN-13: 978-1107060838). With permission.

1.5 L-type voltage-gated calcium-channel (VGCC)

Axonal action potentials (AP) are important for fast inter-neuronal communication. Besides the essential role in action potential initiation and propagation of sodium channels (Huxley 2002), various ion channels also affect the generation of action potentials (Bean 2007). Among these, voltage-gated calcium channels not only participate in intracellular signaling pathways and neurotransmission (Turner et al. 2011), but their activation also seems to modulate other ion channels and has an effect as a vesicular releasing signal of glutamate inside neuronal pre-synapses (Catterall 2011).

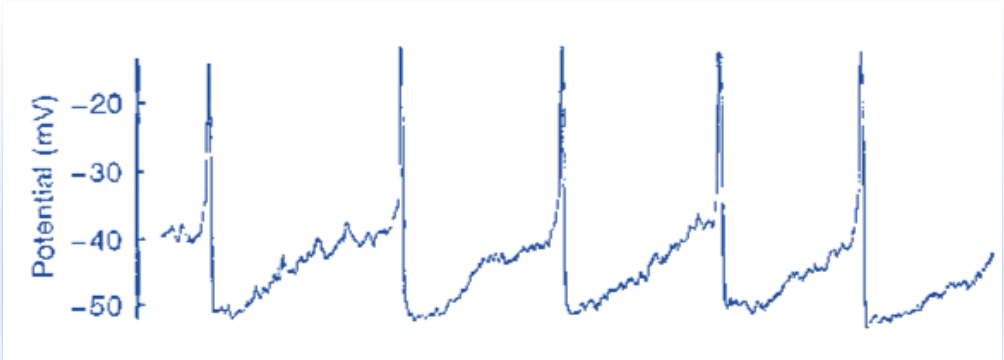

Figure 6. Action potential initiated by calcium influx without participation of sodium. Source: Kwiecien 1998. With permission from Karger AG

Five types of voltage-gated calcium channels (L-, N-, P/Q-, R-, and T-type) with a broad synaptic distribution have been so far identified: in the pre-synapses, calcium-influx appears to be carried by L-type, P/Q- and also R-type channels (Shinnick-Gallagher et al. 2003, Nimmrich and Gross 2012), whereas in the post-synapses, calcium concentration can be modulated through pharmacological blockades of N- and L-type channels (Voglis and Tavernarakis 2006). In comparison to sodium-related activation, L-type voltage-gated calcium channels show slow activation and highly voltage-gated control during potentiation (Kwiecien and Hammond 1998, Lipscombe et al. 2004), as shown in Fig. 6. Additionally, it has been reported that “the contribution of L-type VGCCs to total VGCC currents remained relatively constant” (Morton et al. 2013). In pyramidal neurons, L-type VGCC significantly contribute to the development of

synaptic connections (Kuczewski et al. 2010, Cherubini et al. 2011), and to the modulation of synaptic plasticity (Wolters et al. 2003, Wankerl et al. 2010, Weise et al. 2017) by shifting somatic and dendritic calcium transients (Morton et al. 2013). Pharmacological modulation can be easily established due to their high affinity to dihydropyridines, which suppress almost all possible action potentials for a short period (Kwiecien et al. 1998), as shown in Fig. 7. This study investigates the possible modulation of TMS-induced brain oscillations due to the L-type of VGCCs.

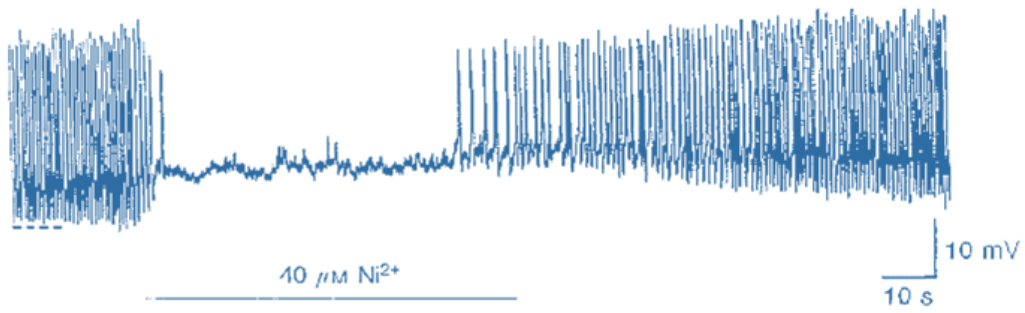

Figure 7. Suppressing action potentials activity by dihydropyridine.
Here: nifedipine on a growth hormone-secreting cell line (GC cell) derived from a rat pituitary tumor. Source: Kwiecien 1998. With permission from Karger AG

1.6 Study Medication

In order to investigate the spectral impact on EEG by modulating the two main glutamatergic receptors and L-type VGCC, we administered perampanel, dextromethorphan and nimodipine as well as placebo in a randomized double-blinded crossover design.

1.6.1 Perampanel

Perampanel, chemically described as 2-(2-oxo-1-phenyl-5-pyridin-2-yl-1,2-dihydropyridin-3-yl) benzonitrile (Satlin et al. 2013) is a highly selective and allosteric antagonist at the AMPAR. It does not interfere with other ionotropic glutamate receptors like NMDAR (Rogawski 2011) and can inhibit all AMPAR-subunits equally, both calcium-permeable and impermeable (Barygin 2016).

According to pharmacokinetic studies, perampanel has an oral bioavailability of almost 100% [1] and its peak plasma concentration can be achieved in approximately 1 hour (Franco et al. 2013), as shown in table 2. As food can delay the T_{max} up to 2 to 3 hours (Tsai et al. 2018), the subjects were asked not to eat during the experimental session. Some trials indicated that more than 90% of oral taken perampanel could be metabolized by type CYP3A4 of liver cytochromes (Patsalos 2015) to inactive metabolites. Multiple interactions with other drugs like other antiepileptic drugs (Patsalos 2015) and alcohol have been reported [2]. The average elimination half-life time ($T_{1/2}$) of perampanel was approximately 105 hrs. (Patsalos 2015, Gidal et al. 2017). Thus, it is necessary to prohibit driving motorized vehicles within 14 days after intake. Female participants were not included due to monthly change of level of progesterone, whose metabolism could be enhanced after application of perampanel 12mg (Patsalos 2015). In therapeutic application, perampanel has been found to be effective in treating partial or generalized tonic-clonic seizures (Krauss et al. 2013, Barygin 2016) and received its renewed approval for patients above 12 years old in Germany since December 2017. Its adverse events concern mainly dysfunction of the central nervous system, for instance, dysbalance, ataxia, dizziness, dysarthria, sleepiness, blurry vision and mental change towards aggressiveness and fear. Vegetative symptoms like higher or lower appetite, nausea and weight gain have also been reported by a multicenter clinical study (Rohracher et al. 2018). The use of Perampanel 12mg was investigated in biopharmaceutic studies[3] and the adverse events at this dosage were considered mild to moderate by Eisai Co. Ltd, which were unpublished at the time of study application and provided after request for permission. Phase-III-studies “demonstrated that once-daily

[1]Source: European Medicines Agency EMA. Perampanel (Fycompa): assessment report (EMA/424476). 2012. Available at: http://www.ema.europa.eu/docs/en_GB/document_library/EPAR_Public_assessment_report/human/002434/WC500130839.pdf. Accessed May 10, 2014.
[2]Source: US Food and Drug Administration FDA. Clinical pharmacology review. Reference ID: 3205587. 2012. Available at: http://www.fda.gov/downloads/Drugs/DevelopmentApprovalProcess/DevelopmentResources/UCM332052.pdf. Accessed May 10, 2014.
[3]Source: Study E2007-E044-037 and E2007-A001-040, CLINICAL PHARMACOLOGY REVIEW from FDA https://www.fda.gov/media/84995/download.

adjunctive perampanel, at doses up to 12mg/day, had a good tolerability profile" (Krauss et al. 2013, Satlin et al. 2013), where more than 91% of patients included in their study received a dosage of 10-12 mg per day. The provided results are now summarized and published in the prescribing information 2016 [4] of Fycompa®.

1.6.2 Dextromethorphan

Dextromethorphan has several functions at different receptor sites inside the CNS. Among many binding affinities (Nguyen et al. 2016), it has been reported that dextromethorphan is mostly affine to the sigma-1-receptor as an agonist, 5-HT serotonin-reuptake receptors as an inhibitor, glycine-receptors as an antagonist and to NMDAR as a non-competitive antagonist (Takahama et al. 1997, Taylor et al. 2016).

Unlike perampanel, dextromethorphan rapidly undergoes a hepatic first-pass effect and is metabolized to its active form – dextrorphan (Capon et al. 1996, Yu et al. 2001). Then, cytochrome P460 (Nguyen et al. 2016) inactivates and decomposes dextrorphan into substances like 3-hydroxymorphinan and demethylation (Yu et al. 2001). The velocity of metabolism is strongly dependent on different CYP2D6-phenotypes of the cytochrome P460 (Woodworth et al. 1987, Capon et al. 1996), which can be generally divided into four classes: ultra-rapid, extensive (normal type), intermediate (reduced activity) and poor metabolizers (Nguyen et al. 2016, Storelli et al. 2018). Different expression of CYP2D6 can dramatically vary the half-life time of dextromethorphan's plasma concentration, from 2.4 hrs for extensive metabolizers to 19.1 hrs, in median for poor metabolizers (Capon et al. 1996), or even extended up to 45 hrs, according to some reports (Pfaff et al. 1983, Schadel et al. 1995). Participants with known intolerance of all substances[5] metabolized by CYP2D6 were not included in the study.

[4]Prescribing information of Fycompa (Eisai Co), see: https://www.accessdata.fda.gov/drugsatfda_docs/label/2016/202834s011lbl.pdf

[5]Relevante substances see: https://www.gelbe-liste.de/arzneimitteltherapiesicherheit/cyp-interaktionen/cyp2d6

Therapeutically, dextromethorphan has been patented as an antitussive drug since 1954, while neuroprotective and anticonvulsive effects have been increasingly revealed in the last two decades (Tortella et al. 1989, Werling et al. 2007, Shin et al. 2011). But dextromethorphan (Dextromethorphan ratiopharm®) can also bring out some adverse events, such as sleepiness, dizziness, nausea to vomiting, and hallucination in rare circumstances[6]. It has been reported that 7% of the population in Germany were poor metabolizers due to the phenotype of CYP2D6 (de Leon et al. 2005). In these cases, a slower metabolization of dextromethorphan can lead to sedation, circulatory collapse as well as the reported general adverse events.

1.6.3 Nimodipine

Nimodipine is a dihydropyridine, which selectively blocks L-type voltage-gated calcium-channel (VGCC) by binding its alpha-1-subunit allosterically (Catterall and Striessnig 1992, Tomassoni et al. 2008). Thus, it limits the influx of extracellular calcium into post-synapses (Igelmund et al. 1996) and keeps the intracellular calcium concentration in a steady state, even under neuronal depolarizing conditions (Tomassoni et al. 2008). In vascular smooth muscle cells, the absence of depolarization results in vasodilatation (Catterall and Striessnig 1992), but in comparison with other dihydropyridines like nifedipine, nimodipine has a quite potent activity in the cerebrovascular system, while only modest activity is detected on peripheral vessels (Tomassoni et al. 2008). Furthermore, it has been shown by some studies that the long-term potentiation is correlated with activation of L-type-calcium channels (Artola et al. 1996, Sjöström and Nelson 2002), and deactivation of L-type-calcium channels by nimodipine can be associated with decreased cortical excitability (Wolters et al. 2003, Wankerl et al. 2010).

The maximum of plasma concentration can be reached between 0.6 and 1.6 hrs. After hepatic-first pass effect, an oral bioavailability of 5-15% has been reported[7], when nimodipine 30mg is applied. Like perampanel, nimodipine is metabolized

[6]Source: Gebrauchsinformation Hustenstiller-ratiopharm® Dextromethorphan.
[7]Source: FACHNFORMATION NIMOTOP® Nimodipine Bayer Resources, https://www.fachinfo.de/pdf/001480

by CYP3A4-type of cytochrome P450 in the liver and excreted partially through a renal and biliary elimination pathway. Therefore, participants with chronic intake of drugs metabolized through CYP3A4, alcohol and grapefruit juice (Hanley et al. 2011) were excluded.

Nimodipine has been shown to be effective in treating vasospasms resulting from subarachnoid hemorrhage (Philippon et al. 1986, Catterall and Striessnig 1992) and cerebral hypertension (Tomassoni et al. 2008). This also implies that nimodipine (Nimodipine Hexal®), as an antihypertensive drug, can cause hypotension. Other minor adverse effects, such as dizziness, flush, headache, nausea, change in heart rate and sweating were also reported by the specialist information on medicinal products [8].

Yet, neuronal effects have been less studied, only anti-seizure efficacy on rats has been indicated by studies in-vivo by some studies so far (Kriz et al. 2003, Shitak et al. 2006).

1.6.4 Placebo

A Placebo is an inert substance, which is available as tablets and capsules in the clinic's drug store of the University of Tübingen. In this study, the application of placebo capsules and tablets aims to ensure the double-blindness of participants and study investigators, as dextromethorphan was only available in capsules, and perampanel and nimodipine in tablets.

1.7 Study motivation and main objectives

Rationale:

Glutamatergic transmission is the major mechanism of excitatory synaptic signaling (Hammond 2015) and GABA is the main representative of inhibitory transmitters of the CNS. Theoretically, it is reasonable to hypothesize that the effect of GABA-agonists on CNS resembles that of antagonists of ionotropic glutamate-related channels and L-type VGCC. While it has been demonstrated that GABA-ergic agonists like baclofen and diazepam can modulate cortical EEG-responses to TMS stimuli (Premoli et al. 2014, Premoli et al. 2018, Tse et al.

[8]Source: Gebrauchsinformation Nimodipin Hexal 30mg

2018), the effect of glutamatergic modulators on TMS-evoked and -induced EEG-responses have not been investigated yet. This study will investigate physiological TMS-induced EEG responses by assessing the excitatory motor system pharmacologically.

Objectives:

1) Investigation of the role of AMPAR- (perampanel) and NMDAR- (dextromethorphan) mediated neurotransmission for resting-state EEG-responses and TMS-induced oscillatory brain activity.

2) Investigation of the role of calcium influx mediated by L-type VGCCs (nimodipine) for resting-state-EEG responses and TMS-induced oscillatory brain activity.

Hypotheses:

Specific hypotheses on this study were not formed as research on pharmaco-TMS-EEG was at its developing state. This study intends to explore and characterize the physiology of resting-state and TMS-induced oscillatory brain activity in response to mediation of the glutamatergic system and L-type VGCCs.

2 Materials and Methods

2.1 Ethics approval

The Approval of the current study was given by the ethics Committee of the Medical Faculty of Eberhard-Karls-University Tübingen (Reg.-No. 526/2014BO1).

2.2 Participants

2.2.1 Subject recruitment

All included participants agreed the in- and exclusion criteria, experimental time plan and procedures by signing a written informed consent form, which includes personal data protection. Furthermore, they were informed about possible adverse events resulting from TMS, EEG and study drugs. They were explicitly informed not to take coffee, grapefruit juice or alcoholic beverage before and during each test session in order to avoid their possible interactions with study drugs and advised not to drive within one week after each test session. All participants received a reimbursement of 50 € for each completed experimental session.

2.2.2 Inclusion criteria

Participants were selected by strict inclusion criteria, which are summarized in the following points:

- aged between 18 and 50 years.
- male subjects. Female subjects were not included due to possible hormonal and blood pressure interactions brought out by the menstrual cycle (Smith et al. 1999).
- right-handed with a laterality score >75% as defined in Edinburgh handedness inventory (R.C.Oldfield 1971).
- free of chronic medication and addictive substances (including alcohol and nicotine).
- no electric or metal implants.
- no history of neurological or psychiatric diseases.

- ❖ no contraindication by any other of the TMS safety requirements (Rossi et al. 2011).

All participants went through a screening procedure of blood pressure and resting-motor-threshold (RMT) measurements. The systolic blood pressure had to be above 100mmHg and RMT is defined as the minimal intensity, which can still elicit MEP with an amplitude ≥50 μV in at least five out of ten stimulations (Groppa et al. 2012, Rossini et al. 2015). Only participants (Rogasch et al. 2013) (mean ± s.d.: 40.38 ± 6,72%) with RMT < 60% of maximum stimulator output (Rogasch et al.) were included. Moreover, their Body-Mass-Index had to be lower than 30 kg/m^2 to avoid possible inequalities of drug concentration, as all subjects received the same drug dosages.

2.2.3 Subjects

Eighteen healthy male participants (mean age ± s.d.: 26.0 ± 3.5 years, range: 22-36 years) participated in the study, and were examined physically and neuro-psychiatrically by a physician of our group. According to the Edinburgh Inventory Test, all participants were right-handed with a mean laterality score ± s.d. of 88 ± 15 %. Among the included participants, one was excluded due to a self-report of hepatitis B infection after beginning of the study and another subject exited the study due to private reasons. The remaining sixteen participants completed all four experimental sessions and their data served as the basis for this thesis.

2.3 Experimental procedures

To assess the glutamatergic system via TMS-EEG, the experiment was designed as a pseudo-randomized and double-blinded crossover study, and completed under four different drug conditions, i.e., perampanel, dextromethorphan, nimodipine and placebo. The interval between two consecutive experimental sessions in a given subject was set to at least 14 days in order to avoid possible carryover effects between sessions. As shown in Fig. 8, each experimental session chiefly consisted of the following four phases:

Initial preparation: Before starting the measurements, participants were told to sit still in a reclining chair. An EEG cap with 64 c-ring-electrodes was placed on their scalp according to the International 10-20 system (Fig. 9, right), and three EMG-electrodes were placed onto the right abductor pollicis brevis (APB) muscle and its adjacent bone to record the EMG- activity, while the third is placed as the ground electrode at the forearm. To minimize the distance between the coil and the scalp, we employed a thin, TMS-compatible cap of 4 mm thickness (Brain Products GmbH). The EMG-electrodes and EEG-electrodes were monitored at their impedance level (Julkunen et al. 2008) by using the software BrainVision Recorder (Brain Products GmbH) and kept lower than 5 kΩ by using appropriate conductive gel at the contact areas of metal and skin.

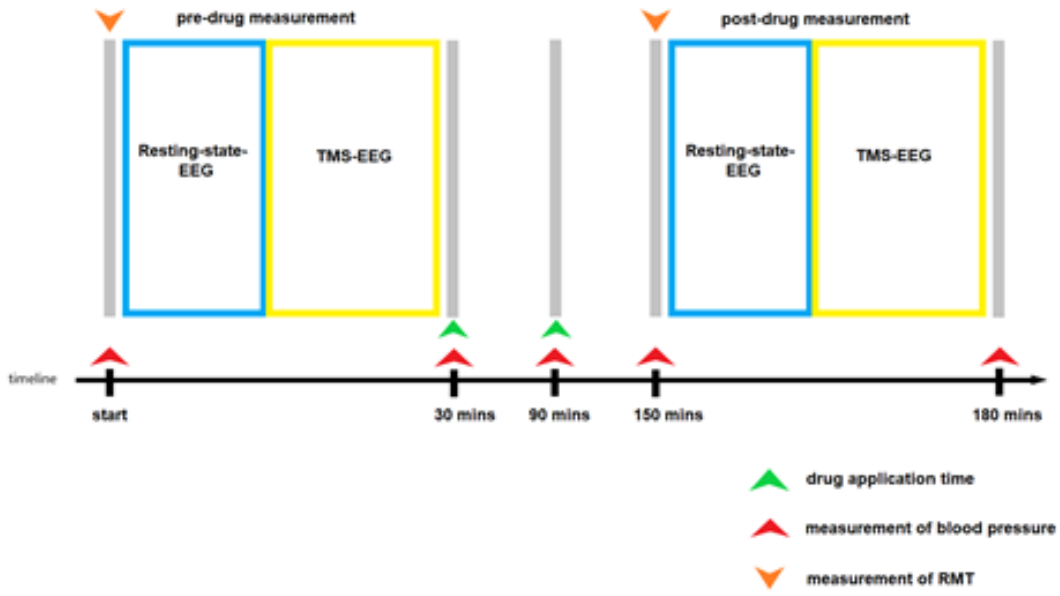

Figure 8. Timeline of an experimental session with marked time-spots.
Red marker: blood pressure measurement; orange marker: measurement of RMT and re-adjustment of hot spot; green marker: drug applications.

After the first measurement of blood pressure, RMT and the TMS hand hotspot (the optimal stimulation site targeting the right APB muscle) were searched manually using a figure-of-eight coil on the left primary motor cortex, mostly enclosing the C3 channel, and then marked out in a tangential T-form onto the EEG cap to maintain the same positioning throughout all test sessions (Fig. 9).

The figure-of-eight coil was kept at a 45-degree angle tangentially to the mid-sagittal line, holding it from behind of the participant (Kammer et al. 2001, Thielscher et al. 2011). The correct targeting of the hot spot has been ensured by monitoring EMG-data using the Spike2 software (Cambridge Electronic Design) throughout the whole session. The recorded data underwent a processing procedure with amplification (Digitimer D360 8-channel amplifier), bandpass filtering (20 Hz – 2000Hz) and was digitized at an A/D rate of 10kHz (CED Micro 1401; Cambridge Electronic Design).

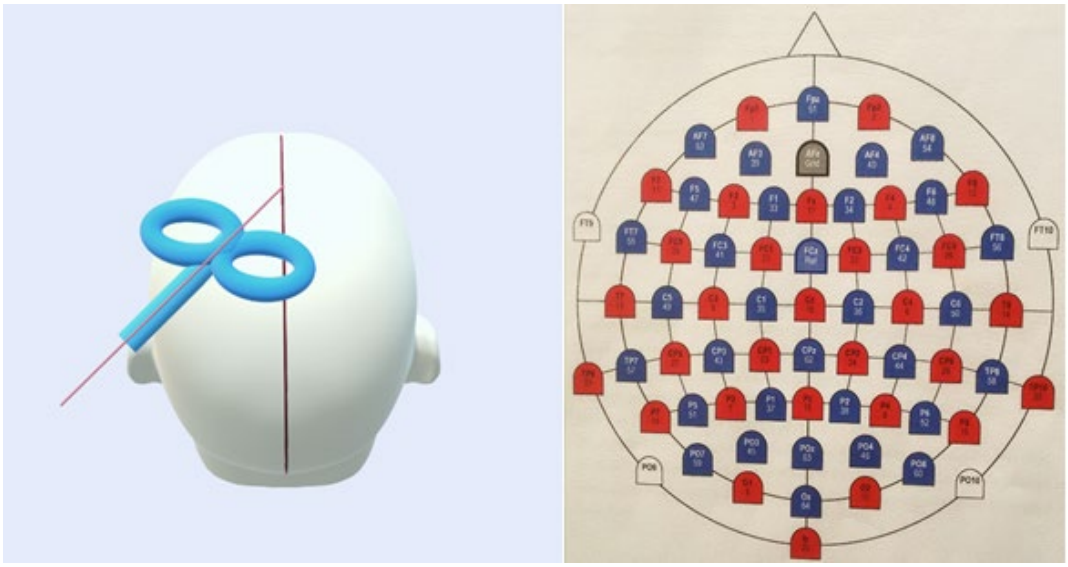

Figure 9. Schematic view of positioning the TMS coil and distribution of EEG electrodes. Left: The angle of the figure-of-8 coil has been held tangentially on the scalp, in a 45-degree angle to the sagittal line; Right: montage of the EEG electrodes in the 64-electrode cap with the ground electrode AFz placed on the forehead as marked grey. Right: product information on www.brainproducts.com).

Subsequently, participant needed to plug in earphones, which sent out a monotone noise, to mask the clicking sound from discharging of the TMS coil, thus minimizing auditory evoked EEG signals (ter Braack et al. 2015). In addition, the participants were told to keep their eyes open, focusing on a marked dot on the wall in front of them to reduce artifacts that were produced by eye movements and blinks.

The subsequent baseline (pre-drug) measurements included two steps: the first was the recording of resting-state EEG, and the second involved TMS-EEG recordings using 150 monophasic single TMS pulses, which has been carried out at an intensity of 100% of measured RMT. Resting-state EEG was recorded for 3 mins. The TMS pulses were applied on the previously marked hot spot by the figure-of-eight coil connected to two MagStim 200^2 magnetic stimulators, while recording EEG-data continuously. The frequency of TMS was computationally set to 0.2 Hz ± 25% random variation. All recorded EEG-raw signals were also amplified, bandpass filtered and digitized at an A/D rate of 10kHz per channel.
Table 1 represents the scheme of drug application. 4 capsules immediately at the end of the pre-drug measurement and 1 tablet 60 mins later were applied each test session to verify the double-blindness and to ensure that the experiment proceeds at the time of maximal plasma concentration of the study drugs (T_{max}), as dextromethorphan has a T_{max} of approximately 2 hours after intake (see Table

Table 1. Scheme of drug application (30 mins after start and 90 mins after start) within the four drug conditions.

Drug condition	First application after baseline measurement	Second application after 60 mins
Perampanel	4x capsules of Placebo	1x tablet of perampanel 12mg or 6mg
Dextromethorphan	4x capsules of Dextromethorphan 30mg	1x tablet of Placebo
Nimodipine	4x capsules of Placebo	1x tablet of nimodipine 30mg
Placebo	4x capsules of Placebo	1x tablet of Placebo

2), while perampanel and nimodipine can reach its T_{max} after 1 hour. The blood pressure of the participants was re-monitored simultaneously to each drug application. As reported in the Table 2, these capsules and tablets included perampanel 12mg/6mg, dextromethorphan 120mg, nimodipine 30mg and

Table 2 Study drugs, brand, dosage and applicated form, time of peak plasma concentrationafter application (T_{max}) and half-life time (T1/2).

Drug and Brand	Dosage	Form	T_{max} [h]	T1/2 [h]
Perampanel (Fycompa®)	12 mg/ 6 mg	tablet	0.5-4 (**1**)[1]	105[1]
Dextromethorphan (Hustenstiller-ratiopharm® Dextromethorphan)	120 mg	capsule	1-**2**[2]	1.2-2.2 hrs.[3] (CYP2D6-EM) or < 45 hrs.[3] (CYP2D6-PM)
Nimodipine (Nimodipin-HEXAL®)	30 mg	tablet	0.6-1.6 (**1**)[4]	1.1-1.7[4]
Placebo tablets (P-Tabletten Lichtenstein, 7, 8, 10 mm, Winthrop)	n.a.	tablet	n.a.	n.a.
Placebo capsules (Universitäts-apotheke)	n.a.	capsule	n.a	n.a

Average T_{max} time were taken in consideration for study design and marked bold in baskets. CYP2D6-PM: poor metabolizer of CYP2D6. n.a: not applicable.

Source of literature:

1) Tmax data is provided by Phase I randomized biopharmaceutical study E2007-A001-040 and -037 after communication with Eisai Co. With permission; T1/2 data is based on Gidal et al 2017, Patsalos et al. 2014.
2) PRODUCT INFORMATION Hustenstiller-ratiopharm® Dextromethorphan for CYP2D6-extensive metabolizer (CYP2D6-EM).
3) Woodworth et al., 1987; Pfaff et al. 1983, Schadel et al. 1995 for CYP2D6-poor metabolizer (CYP2D6-PM).
4) FACHNFORMATION NIMOTOP® Nimodipine Bayer Resources.

placebo, respectively. Of note, the dosage of perampanel was reduced due to drug-related adverse events during the course of this project. Perampanel 12mg was only used to the first three participants.

For the post-drug measurement, the conductivity of all prepared EEG- and muscle electrodes was re-tested and re-optimized by using conductive gel. The RMT was re-measured in the same way as mentioned above. The intensity of each TMS-pulse has been adjusted to 100% of the re-tested RMT. In addition, the blood pressure of the participants was measured again. Subsequently, the post-drug measurements (resting-state EEG, TMS-EEG) were analogous to the baseline measurements (Fig. 8).

As a last step, a safety check was performed: a neurological examination and a last blood pressure measurement were administered by a physician. The neurological examination contained clinical tests of cranial nerves II – XI, gait pattern and ability of balancing like a tightrope walk, and Romberg's test.

2.4 Used non-drug materials

- An automatic blood pressure measurement device.
- TMS magnetic stimulators: two MagStim 200 magnetic stimulators connected to one figure-of-eight coil with external loop diameters of 90 mm through a BiStim module (all devices from Magstim Co, Whitland, Dyfed, UK). We used two stimulators to prevent overheating events.
- TMS-compatible EEG equipment: A 64-electrode cap and three Ag-AgCl-cup electrodes for EMG measurement, BrainAmp DC, BrainVision Recorder Software, by Brain Products GmbH, Munich, Germany.
- An isolated D360 Amplifier system with band filtering function from Digitimer Ltd. Hertfordshire, UK.
- A Digitizer: Micro1401 mk II from CED Cambridge Electronic Design, Cambridge, UK.
- Conducting gel: Nuprep Skin Prep Gel from Weaver and Company, Colorado, USA and electrode paste from GE GmbH, Freiburg, Germany.

2.5 Data Processing

EEG data processing was performed with Fieldtrip open source-toolbox scripts by using MATLAB R2016a (Oostenveld et al. 2011).

2.5.1 Resting-state oscillations

First, the raw resting-state-EEG data were cut into time segments of 2 s, bandpass filtered by a zero-phase Butterworth filter of the 3rd order from 1 to 80 Hz and down-sampled to 1000 Hz. 50 Hz artifacts induced by the power line (Freche et al. 2018) were notch-filtered by using the same filter system at 49-51 Hz. A mean (± s.d) of 5 (± 2) Channels and 14.6 (± 8.9) % of epochs containing visual detectable noises were removed by individual and manual selection. Subsequently, the data underwent an independent component analysis (ICA) by means of the FastICA algorithm (Rogasch et al. 2014). Identifiable ICA components (mean ± s.d. 18 ± 4) contaminated by artifacts, which resulted from eye and lid movement, facial and masticatory muscle activity were removed on the basis of their power spectrum, topographical specification and single-trial time-course. Then, the data of discarded channels were re-calculated by spline-interpolation of adjacent channels (Perrin et al. 1989, Thut et al. 2011). The resulted data were re-referenced on the average reference signal. A fast Fourier transform (FFT) algorithm, with a spectral resolution of 1 Hz and smoothing ±1/4 of the central frequency, was applied for all epoched data of each EEG channel with a power spectrum from 1 Hz to 45 Hz by using multi-taper method (Babadi and Brown 2014), implemented in the Fieldtrip toolbox (Oostenveld et al. 2011). The pre-processed data were averaged over all retained epochs of either pre- or post-drug data.

2.5.2 TMS - induced oscillations

The raw TMS-EEG data were also cut into epochs in relation to the time of the TMS pulse. Data from 600 ms before to 600 ms after the TMS trigger were considered for further processing, while the data contaminated by the TMS artifact from 1 ms before to 15 ms after the TMS pulse, were removed. The data gap was cubic spline interpolated. Noisy channels (mean ± s.d.: 5 ± 3) and the

epochs (25.4 ± 12.0%) containing visually detectable disturbances were discarded. Differently from the resting-state EEG processing, the ICA was applied in a two-step procedure. In the first ICA step, components (mean ± s.d. of 4.3 ± 2.6) related to TMS discharging artifact, which causes a high amplitude as representatively shown in Fig. 10, were removed.

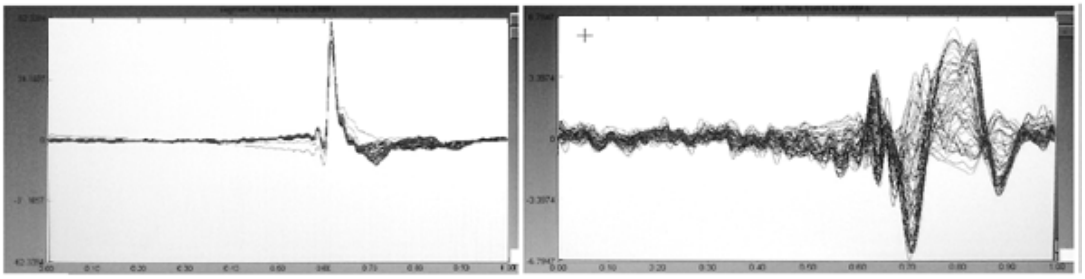

Figure 10. Demonstration of first step ICA during data processing of one representative session.
Left: raw data example of one experimental session before first ICA analysis of all channels. Right: after discarding ICA components related to the high amplitude artifact of TMS stimulation.

After the first ICA, the data were filtered by using a 1 - 80 Hz bandpass filter (zero-phase Butterworth, 3rd order) and a 49 - 51 Hz notch filter (zero-phase Butterworth, 3rd order), followed by data down-sampling to 1000 Hz. In the second ICA, artifact-contaminated ICA components caused by eye and lid movement, facial and masticatory muscle activity were removed analogously to the resting-state data and re-referenced to average reference signal (Rogasch et al. 2014).

The data after removing artifacts were still a mixture of TMS-evoked time-locked responses and TMS-induced spontaneous brain EEG activity (Roach and Mathalon 2008, Herrmann et al. 2014, Pellicciari et al. 2017), which are non-time-locked to the stimulus onset. The induced activity has been isolated in the time-domain by channel-wise subtracting the average evoked response from each single trial (Premoli et al. 2017). Subsequently, a convolution of single trials with complex Morlet wavelets were used to calculate time-frequency representations (TFRs) of the obtained data (Wacker and Witte 2013) in the frequency range from

6 to 45 Hz in step of 1 Hz, while the center of the wavelet was shifted in step of 10ms in the time window - 600ms to 600ms related to TMS application. The length of the wavelet was linearly increasing from 2.5 cycles at 6 Hz to 7.5 cycles at 45 Hz (Cohen 2019). Squared values of the complex time series preprocessed with wavelet transformation were taken as power of TFR. A trial-wise z-transformation has been performed based on the mean and standard deviation of the full-length trial as described in (Roach and Mathalon 2008) and their baseline was corrected subtracting the mean value (over time) of the baseline period (from 300 ms to 100 ms before TMS), to ensure that the average pre-TMS values were unequal to zero, so that z-values can be interpreted as a modulation of the pre-TMS oscillatory activity. Finally, TFR was averaged over all obtained epochs for pre- or post-drug data and additionally trimmed, so that the marked time points without time-frequency values can be removed (from - 600 to – 400 ms before and from 400 to 600 ms after the TMS-stimulation point, corresponding to 1.25 cycles of the 6 Hz oscillation at the beginning and end of the epoch).

2.6 Statistical Analysis

The analysis of obtained EEG data have been further performed with Fieldtrip open source-toolbox scripts by using MATLAB R2016a (Maris and Oostenveld 2007, Oostenveld et al. 2011). For analysis of the RMT, a repeated-measures analysis of variance (rmANOVA) within subjects concerning two factors, DRUG (4 levels due to four condition groups) and TIME (2 levels: pre-drug vs. post-drug), has been used to detect possible changes. An applied Kolmogorov-Smirnov-Lilliefors-Test did not detect any deviation from a normal Gaussian distribution, while sphericity was tested using Mauchly's test. All discrepancies were corrected using the Greenhouse-Geisser method, resulting in an epsilon-value less than 0.75. Two-tailed paired t-tests with a significance level set to $p < 0.05$ were applied when statistically significant main effects or interactions were detected.

2.6.1 Resting-state oscillations

Frequencies of interest (FOI) were selected in the most common band widths: delta (1 – 3 Hz), theta (4 – 7 Hz), alpha (8 – 12 Hz), beta (13 – 30 Hz) and gamma

(31 – 45 Hz). Gamma-band with frequencies > 45 Hz were excluded from statistical analysis, in order to reduce high-frequent noise interactions induced by power lines and other electrical devices around 50Hz (Light et al. 2010). To ensure the reproducibility, all pre-drug data were statistically compared across all experimental conditions. Post-drug data were compared with corresponding pre-drug data in cluster-based t-tests for each drug condition and each FOI. The obtained p-values underwent a Bonferroni-correction to adjust for multiple comparisons. In addition, power values of each post-drug test condition were calculated by subtracting pre-drug condition in order to detect absolute differences.

2.6.2 TMS - induced oscillations

For the analysis of time-frequency power spectra of TMS-induced oscillations (Premoli et al. 2018), two time-regions of interest (TOIs) were defined as an early and a late response (30 - 200ms and 200 - 400ms, respectively) in the frequency band widths where drug-related changes were most expected, i.e., the alpha and beta frequencies (Jensen et al. 2005, Neuper et al. 2005, Engel and Fries 2010), as shown in Fig. 11. Then, we extended the analysis and integrated delta, theta and gamma frequency bands into the defined TOIs (Roach and Mathalon 2008, Jensen et al. 2014, Monsalve et al. 2018). Frequencies < 4 Hz within delta-band were not included, as these frequencies are not available in the selected time epochs (- 600 ms to 600 ms), and changes in these regions are less expected to be significant (Roach and Mathalon 2008). High frequencies (> 40 Hz) were not included due to TMS-recharging artifact at 200 ms (Veniero et al. 2009) and electrical noise around 50 Hz due to power supply and other electrical devices (Light et al. 2010), as shown in the thick-lined black boxes in Fig. 12.

For reproducibility, the induced oscillation data were statistically compared across all pre-drug conditions. Subsequently, the power of TFR were statistically evaluated between post- vs. pre-drug data for each region of interest. Significant statistic FOI underwent a channel-wise paired t-test for each time-frequency region under all conditions for pre-drug measurement. A cluster-based

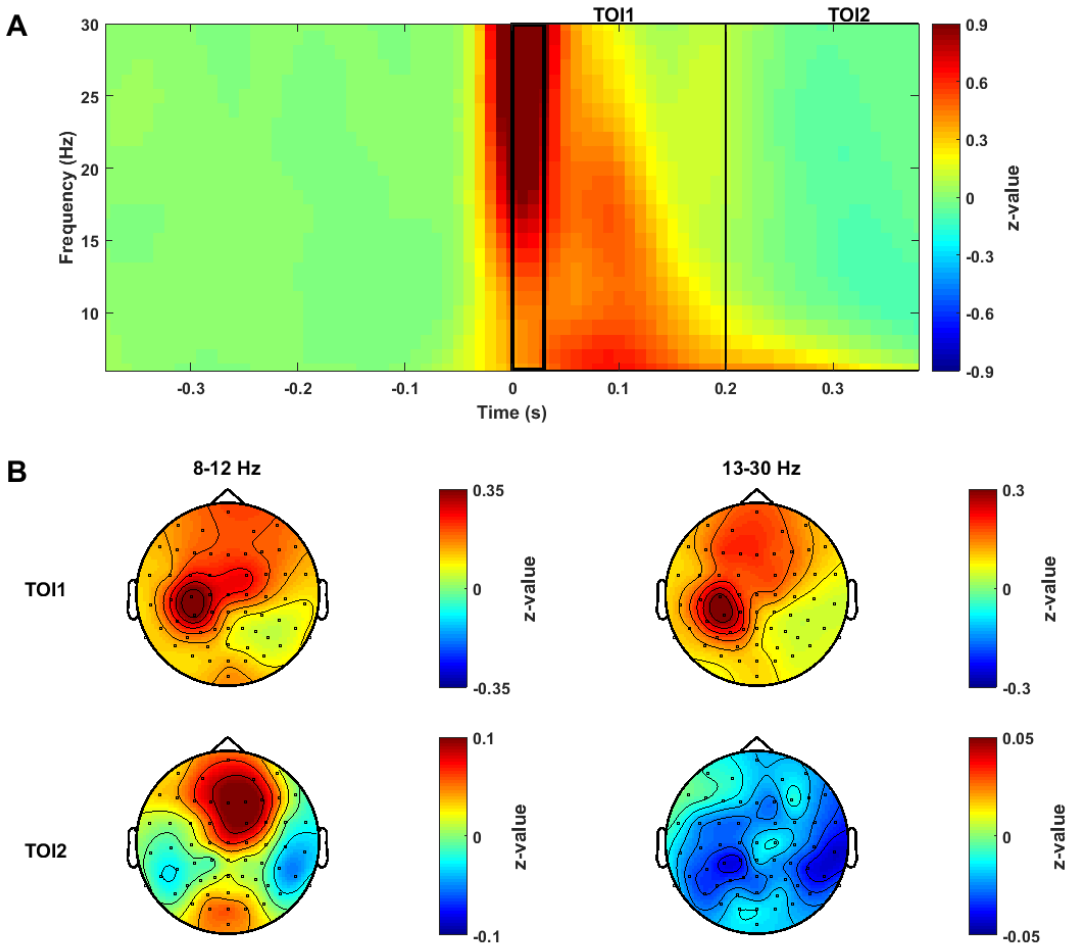

Figure 11. Choice of time regions of interests (TOIs) in a time-frequency representation.

A: choice of early response from 30-200ms and late response from 200-400ms within 30Hz. Black box indicates TMS artifacts from 0 -30ms after stimulus and has been discarded from analysis.

B: topographical presentations of early responses dived by two frequency bands: alpha (left) within 8-12Hz and beta (right) within 13-30Hz. Power spectra are indicated as z-values in the right color bars.

permutation approach[9], which was implemented in Fieldtrip, has been performed at a defined threshold $p < 0.05$, formed by clusters of at least two adjacent channels. T-statistics has been established by summarization of t-values within each cluster comparing the maximum of the obtained t-values (Pernet et al. 2015). The same approach, with 1500 randomizations performed between each two

[9]Source of instructions: http://www.fieldtriptoolbox.org/tutorial/cluster_permutation_freq/

conditions, was taken as the reference distribution of the maximum of the obtained t-value. Like in the resting-state EEG data analysis, Bonferroni-correction was applied to the p-values across all pre-drug experimental sessions. Topographical distribution within defined band widths were displayed in relation to early and late responses.

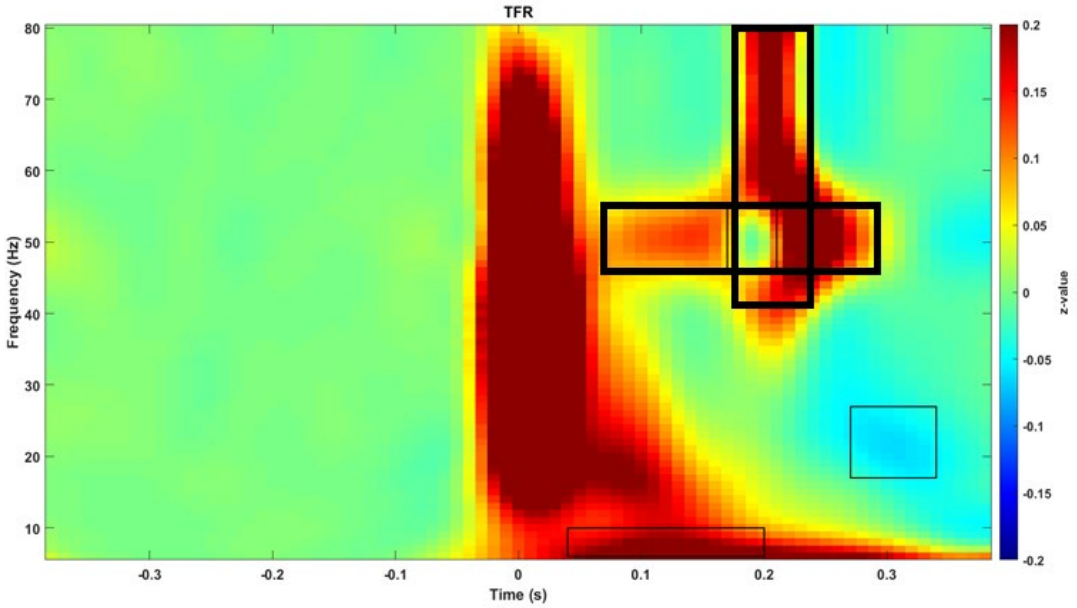

Figure 12. Example of TMS-related artifact in Time-frequency-representation including frequencies above 40 Hz.
TFR has been created after averaging over all pre- and post-drug conditions and subjects. Boxes with thicker black line indicate related artifacts with great potential of contamination. Boxes with thinner black line show possible TMS-induced changes in power.

3 Results

3.1 Drug tolerance

During the experiments, only minor adverse events were reported in relation to TMS, e.g. headache, acoustic irritation by TMS-clicking and paresthesia, which remitted on the same day. Possible allergic reaction to the conducting gel, paste and EEG-electrode material was not observed during the whole study.
After intake of perampanel 12mg, three participants in our study reported side effects (dizziness, sleepiness, severe ataxia and paresthesia in different locations lasting longer than 4 hrs). Thus, we decided to lower the study dosage of perampanel to 6mg for all of the following participants. After the dosage reduction, relevant adverse events were no longer observed. Only mild symptoms, such as dizziness in 7 cases, hypesthesia on fingertips and tongue in 2 cases, were reported and did not last beyond the experimental session. Also, as participants who reported to have drug intolerance to CYP2D6-affine medication[5] were not included, only mild adverse events like dizziness and nausea were noted in 5 subjects after dextromethorphan intake. A significant hypotension due to nimodipine has not been observed. Only one subject showed slight dizziness and unsteady gait, and another subjects self-reported slight increase of forgetfulness. None of the reported drug-related adverse events lasted beyond the same day of application.

3.2 Resting-motor threshold

In the pre-drug measurements, the mean value (± s.d. in percentage of MSO) of RMT was 40.0 (± 6.4%) for perampanel, 40.9 (± 7.5%) for dextromethorphan, 40.4 (± 7.2%) for nimodipine and 40.8 (± 5.8%) for placebo, respectively. Whereas in the post-drug measurement, its mean value (± s.d.) was 43.6 (± 7.6%) for perampanel, 40.4 (± 6.7%) for dextromethorphan, 41.8 (± 7.1%) for nimodipine and 38.7 (± 8.3%) for placebo. By means of rmANOVA, a significant DRUG x TIME interaction was demonstrated ($F_{3,45} = 8.993$, $p < 0.001$), and a series of pairwise post-hoc comparisons between pre-drug and post-drug conditions revealed a significant increase of RMT after intake of perampanel ($p <$

0.001) and nimodipine ($p = 0.0037$). No significant changes in RMT were observed in the dextromethorphan and placebo sessions (König et al. 2019).

3.3 Resting-state oscillatory EEG responses

Across all pre-drug sessions, no significant clusters were observed in pre-drug resting-state EEG oscillatory power, and there were no differences for the placebo session in post- vs. pre-drug condition. This confirms stability of the obtained resting-state EEG data.

Compared with pre-drug resting-state EEG oscillations, post-drug resting-state EEG oscillations showed significant increases in power in all tested frequency bands except the gamma-band (delta, theta, alpha, beta and theta wavelets with p-value <0.001, see Fig. 13) after intake of perampanel. The topographic distribution of power differences was quite unspecific across the channels across all significant frequency bands.

As shown in Fig. 13, after application of dextromethorphan, the power was significantly increased in the gamma frequency band up to 45Hz with $p < 0.002$. The significant clusters are topographically distributed in all brain region except the stimulated area and the contralateral occipital area.

Nimodipine significantly increased power in beta and gamma bands ($p < 0.05$). The topographical distribution of these changes was localized mainly in the hemisphere contralateral to the stimulation site (Fig. 13).

Perampanel
Dextromethorphan
Nimodipine
Placebo
Delta
1-3 Hz
Theta
4-7 Hz
Alpha
8-12 Hz
Beta
13-30 Hz
Gamma
31-45 Hz
POST-PRE
STAT
ΔμV²
t-value
p < 0.001
p = 0.03
p = 0.002

Figure 13. Topographical distribution of resting-state EEG-oscillatory responses in comparison between pre- and post-drug divided in analyzed frequency bands and drug condition.
Power of TFR has been colored from red (above zero) to blue (below zero) as t-value in continuous intensity. Upper row of each frequency band (POST-PRE) shows absolute power changes subtracting pre-drug- from post-drug power values. Statistical differences are shown in the lower row of each frequency band, where significant areas are indicated channel-wise as black dots with corresponding p-value of the significant cluster.

3.4 TMS- induced oscillatory EEG responses

Similarly, there were no significant clusters across the pre-drug conditions and between post- and pre-drug condition of the placebo session in all clusters of the time-frequency-regions of interest (all $p > 0.05$, see Fig. 14). In this way, reproducibility of obtained TMS-induced oscillatory EEG data was also demonstrated.

Although the resting-state EEG data showed significant changes (see above, and Fig. 13), neither of the three post- vs. pre-drug conditions (perampanel, dextromethorphan and nimodipine) could statistically confirm a difference within the tested frequency bands (Fig. 14). However, the power distribution of the tested time-frequency responses changed from early (30-200ms after stimulation) to late (200-400ms after stimulation) oscillatory response. This was visualized in two steps: an early power increase, followed by a late power decrease (see Fig. 14), also demonstrated by a previous study (Premoli et al. 2017). Figure 15 shows channel-wise averaged time-frequency presentations across all four drug conditions including data before and after drug application, but before exclusion of the data above 45Hz. Still, after extension of the analyzed frequencies onto theta- and gamma-frequency bands, a cluster-based statistical power difference could not be found, see topography plots in Fig. 16.

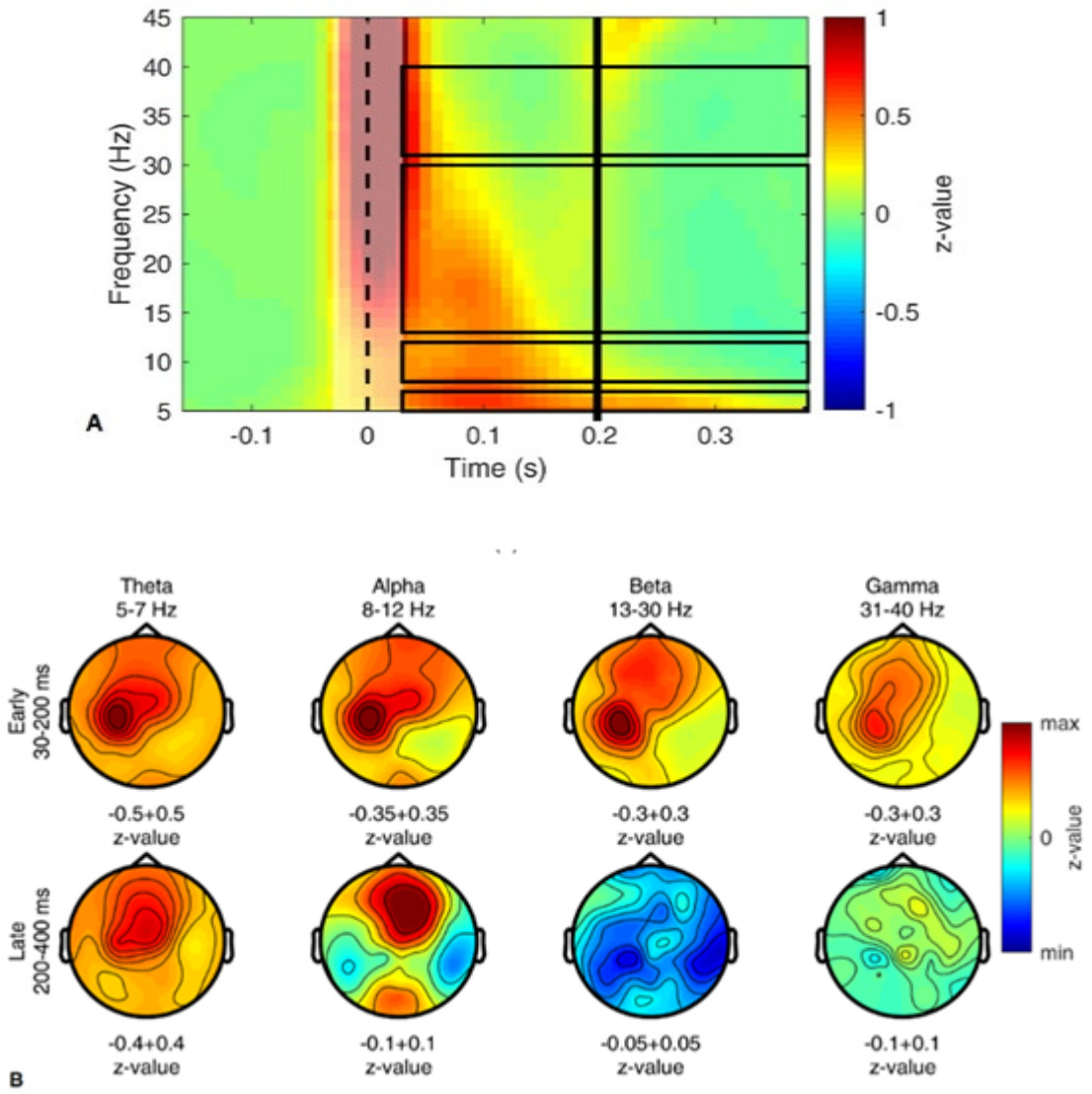

Figure 14. Average time-frequency-representations of TMS-induced EEG oscillations across all pre-drug conditions.

A: Average Time-frequency-representation on channel C3 across subjects and pre-drug conditions of TMS-induced EEG oscillatory responses. Dashed line represents the TMS pulse as a zero-reference for Time. Analyzed early (from 30 to 200ms) and late (from 200 to 400ms) time-frequency regions of interest are divided by middle black line at 200ms post-stimulus. Marked area by black blocks represent the analyzed frequency band widths (theta (5-7Hz), alpha (8-12Hz), beta (13- 30Hz) and gamma (31-40Hz).

B: Topographical distribution of frequency-representation divided in early (upper row) and late (lower row) time-regions. Z-value for power has been colored red (above zero) to blue (below zero) with continuous intensity.

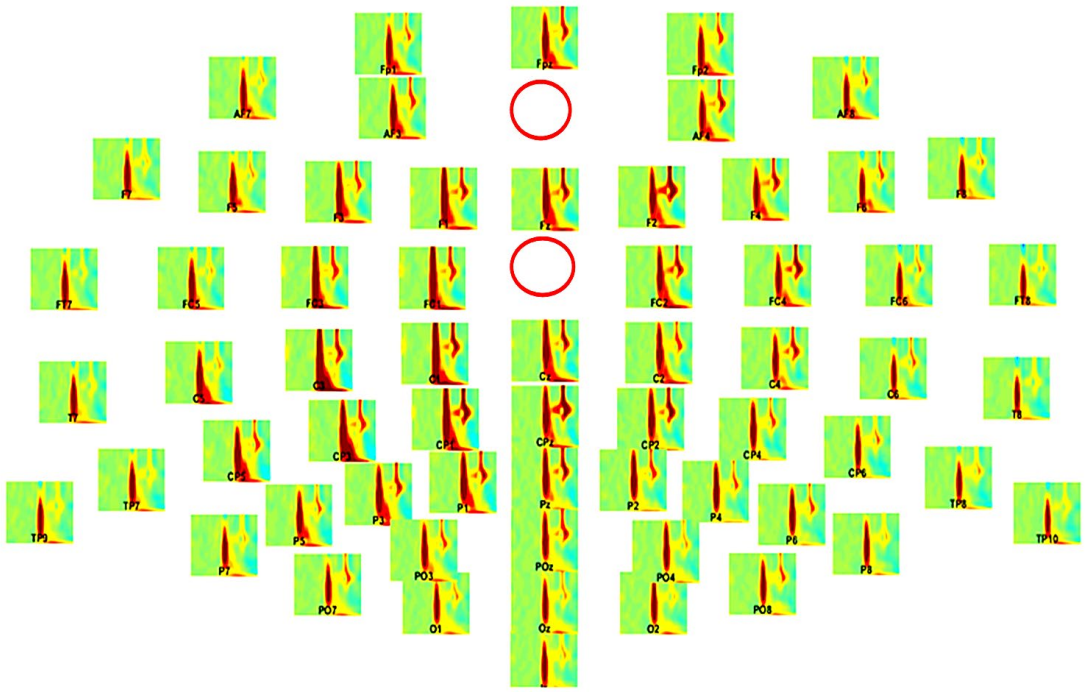

Figure 15. Distribution of channel-wise averaged TFR across all pre- and postdrug condition for all subjects.
Red circled areas mark the missing channels “AFz” (ground electrode) and “FCz” (reference electrode). TFR are shown in small pictures to visualize channel-wise differences, x-axis: time in ms, y-axis: frequency in Hz, corresponding to figure 17.

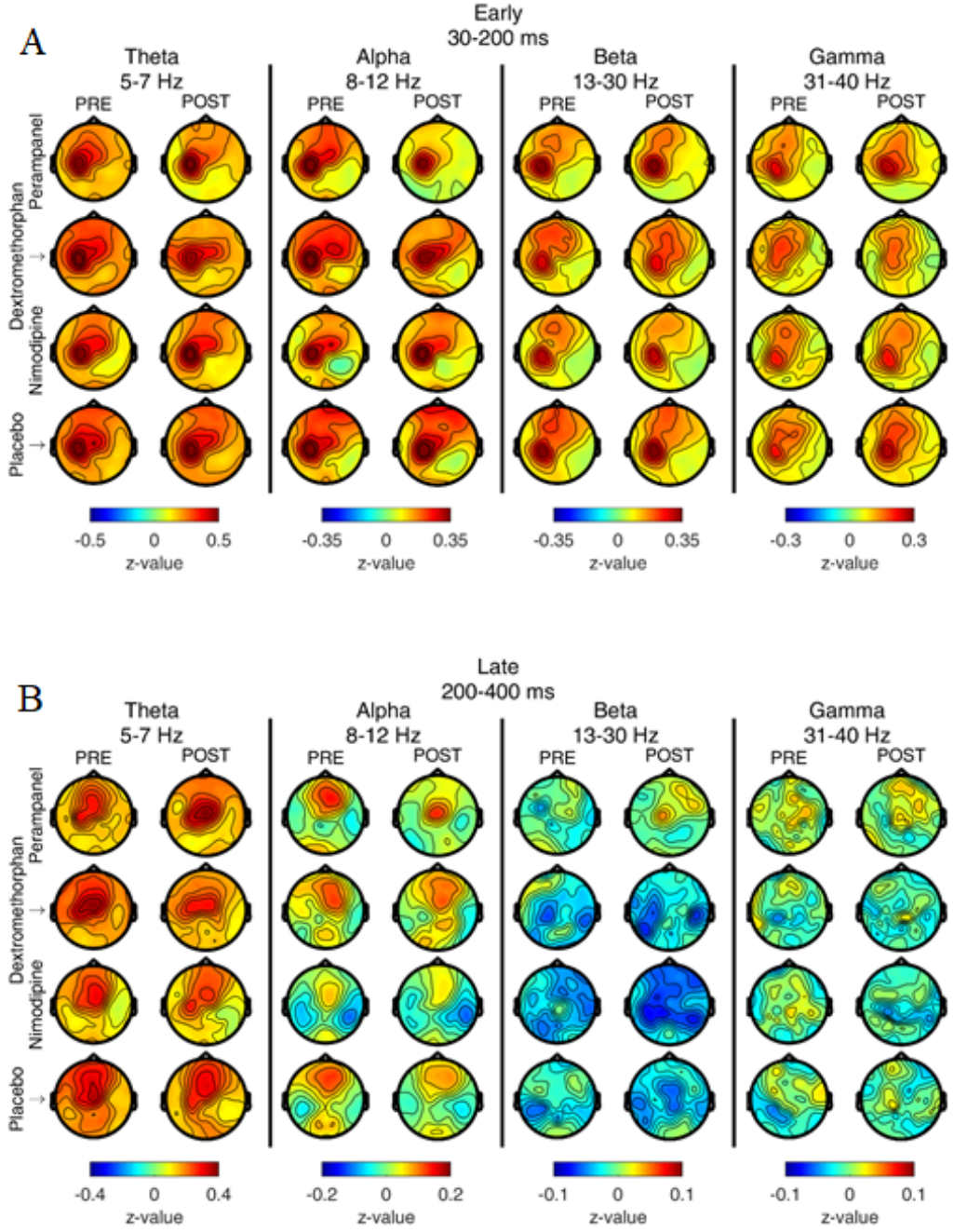

Figure 16. Topographical power distribution (z-value) of time-frequency representations of TMS-induced EEG oscillatory responses.
Divided in early (A: 30-200ms post stimulus) and late time-regions (B: 200-400ms post stimulus). Z-values in all eight time-frequency-regions are colored from red (above zero) to blue (below zero) with continuous intensity. Rows represent the applied four drug-conditions and Columns pre- or post-drug topographical power distribution within the defined frequency band widths (theta: 5-7Hz, alpha: 8-12Hz, beta: 13- 30Hz and gamma: 31-40Hz). No cluster-based statistical difference could be found between post-drug vs pre-drug TMS-induced oscillatory responses.

4 Discussion

In this study, we investigated the effect of two anti-glutamatergic drugs and a VGCC-blocker on resting-state EEG and TMS-induced EEG oscillations. The results may bring a new analytic insight into the connection between pharmacological modulation, resting and induced oscillatory brain activity in the excitatory system.

4.1 Resting-state oscillations

4.1.1 Enhanced Δ, θ, α and β-synchronization after application of perampanel

With respect to the AMPA-system, perampanel does not only lead to a significant increase of RMT, but also to a decrease of TMS-evoked EEG responses, especially the amplitude of P70 (König et al. 2019). Despite clear TEP modulation, perampanel significantly increases power of all frequency-bands except for gamma-oscillations in the resting-state EEG. However, concerning the TMS-induced spatio-spectral profile of cortical oscillations, there were discrepant findings. On the one hand (Premoli et al. 2017) showed significant effects on TMS-induced oscillations effects by applying GABA-ergic drugs, specifically a decrease of alpha-oscillations by baclofen and an increase of beta-synchronization by alprazolam and baclofen. On the other hand, no statistical effect on TMS-induced oscillations could be observed after application of perampanel and dextromethorphan. Possible explanations for the discrepancy are discussed in the following:

Firstly, when comparing post-drug- with baseline-RMT, a significantly higher intensity is needed to elicit MEP (König et al. 2019) after application of perampanel, which indicates a reduction of corticospinal excitability.

Secondly, the action potentials of glutamatergic transmission include currents mediated through two different receptors: AMPAR and NMDAR. AMPAR-related transmission is commonly related to faster kinetics than that of NMDAR, not only with regard to fast EPSPs, but also with regard to fast desensitization (Clements et al. 1998). Such fast kinetics in excitation can create more frequent spiking,

which can generate more action potentials within a shorter period. These higher firing rates may be involved in processes such as active thinking and movement execution that are related to gamma-band oscillations (Muthukumaraswamy 2010). (Teleńczuk et al. 2015) correlated spiking activity of cortical neurons as primary origin of high-frequent EEG. After antagonizing AMPARs, it can be asserted that only slower excitatory activations by NMDAR-related transmission are left over that have a longer decaying time over hundreds of milliseconds (Lester et al. 1990), thus resulting in slower frequencies (Rogasch et al. 2019). Our results are consistent with a recent pharmacological in-vitro study, which presented a significant power increase of slow oscillations like theta-band, when non-competitively blocking AMPAR by SYM2206 (Johnson et al. 2017). Furthermore, Johnson and colleagues also reported an increased power in gamma-oscillation when applying SYM2206. According to their explanation, the mechanism of the increased power of gamma-oscillations was entirely separated to the mechanism of other frequencies (Johnson et al. 2017). This is consistent with other study using in-vivo magnetoencephalography, which showed significant increases in lower frequency power (delta, theta, alpha and beta) after application of perampanel 6mg (Routley et al. 2017). These results are mostly in line with our findings. It should be noted that only frequencies below 45 Hz were evaluated in our study after artefact rejection, so that no change of gamma-oscillations could be found in contrary to the results of (Muthukumaraswamy et al. 2016), who observed a decrease of gamma-frequencies from 30 Hz to 80 Hz, and (Routley et al. 2017), who described a decrease of gamma-frequencies from 50Hz to 90Hz.

Thirdly, AMPAR-mediated EPSC in interneurons can disrupt synchronization of gamma-oscillations, as demonstrated by an in-vitro study (Fuchs et al. 2001), where the interneurons with AMPA-subunit GluR2 were genetically over-expressed. When antagonizing AMPARs by applying perampanel, both AMPAR-related pyramidal neurons and AMPAR-containing interneurons should be less activated, leading to lower activation not only of the AMPA-related excitatory system, but also the AMPA-related inhibitory system of interneurons (Jang et al. 2015). This co-activation of both excitatory and inhibitory systems could partially

Table 3. Spectral cortical responses to AMPAR antagonists using different methods.

Used drug	Author	RMT	Resting-state outcome	Main outcome after event trigger/ stimulation type
Perampanel	(Muthukumaraswamy et al. 2016)		Ø α, 🡻 γ (30-80Hz)	in vivo by magneto-encephalography
SYM2206 (non-competitive)	(Johnson et al. 2017)	-	🡹 θ, γ	in-vitro
Perampanel	(Routley et al. 2017)	-	🡹 Δ, θ, α, β 🡻 γ (50-90Hz)	in vivo by magnetoen-cephalography
Perampanel (allosteric, non-competitive)	current study	🡹	🡹 Δ, θ, α, β Ø γ (< 45Hz)	Ø all frequencies (single-pulse TMS) 🡻 P70 (single-pulse TMS)

- incompatible method or not tested, 🡹 increase, 🡻 decrease, **Ø** no significant changes. Δ deta-band, θ theta-band, α alpha-band, β beta-band, γ gamma-band.

neutralize the excitatory effects. This may explain why AMPA-related gamma-oscillations remain without significant change after perampanel intake in the resting-state EEG in our study.

The significant increase of RMT after perampanel needs to be related to the consistent absence of RMT changes in previous studies after modulation of the NMDAR-dependent glutamatergic system by dextromethorphan (Ziemann et al. 1998, Veniero et al. 2009, Wankerl et al. 2010, Johnson et al. 2017, Rogasch et al. 2019), see Table 4. Thus, it can be concluded that AMPAR-related glutamatergic activation plays an essential role for corticospinal excitability, whereas NMDAR-related activation is subordinate regarding the RMT.

4.1.2 Increased γ -oscillations after application of dextromethorphan

Dextromethorphan as a NMDAR antagonist can suppress excitatory drive and plays an important role in cortical inhibition (Church et al. 1985, Ziemann et al. 1998, Wankerl et al. 2010), but compared with AMPAR-related transmission, its most remarkable features are slower kinetics and longer desensitizing time. Therefore, power of higher frequency oscillations is possibly enhanced after application of dextromethorphan, represented by an increase of power of gamma-frequencies of resting-state EEG in our study, as only AMPAR-related excitatory transmissions remain. This result is in line with other in-vitro studies (Pinault 2008, Hakami et al. 2009, McNally et al. 2011), in which a significant effect of synchronization in gamma-frequencies (Johnson et al. 2017) has also been monitored after intake of the non-competitive NMDAR-inhibitor “MK-801”, ketamine and another non-specific non-competitive NMDAR antagonists.

Another interpretation of gamma-power enhancement at rest was suggested by Korotkova and colleagues who also reported findings of enhanced gamma-oscillations at resting-state after dextromethorphan intake. Similar to the AMPAR-related interneuronal transmission, dextromethorphan also can inhibit NMDA-affine interneurons in hippocampal CA1, leading to enhanced excitability in pyramidal neurons and synchronization of gamma-oscillations (Korotkova et al. 2010).

It is worth noting that another work reported different observations. According to Rogasch (Rogasch et al. 2020), after intake of dextromethorphan, the delta and theta oscillatory power were reduced in resting-state EEG, whereas gamma-oscillation power did not increase. This difference between those and our results lies probably in the difference between measurement times (60 min in the Rogasch study vs. 120 min in our study) after intake of dextromethorphan. This could mean that the influence of plasma concentration of dextromethorphan on the variation of neuronal excitability is non-negligible, as it has an early effect on lower frequencies (decrease of delta and theta) and a late effect on higher frequencies (increase of gamma).

Table 4. Spectral cortical responses to NMDAR antagonists using different methods.

Used drug	Author	RMT	Resting-state oscillations	Main outcome after event trigger/ stimulation type or protocol
Dextromethorphan	(Ziemann et al. 1998)	Ø	-	↑ intracortical inhibition (ICI) ↓ intracortical facilitation (ICF)
Dextromethorphan	(Wankerl et al. 2010)	Ø	-	↓ facilitation and ↑ depression of induced enhancement by theta-burst stimulation
Dextromethorphan	(Korotkova et al. 2010)	Ø	↑ γ	(Selective ablation of NMDARs in animal study)
MK-801 (non-competitive)	(Johnson et al. 2017)	-	↑ γ, θ	(in-vitro)
Ketamine (non-competitive)	(Johnson et al. 2017)	-	↑ γ, θ	(in-vitro)
unspecified competitive antagonist	(Johnson et al. 2017)	-	↑ γ Ø θ	(in-vitro)
Dextromethorphan	(Salavati et al. 2018a)	-	-	↓ LTP (PAS)
Dextromethorphan	(Salavati et al. 2018b)	-	-	Ø LICI
Dextromethorphan	(Hui et al. 2020)	-	-	Ø ISP after single pulse TMS
Dextromethorphan	(Rogasch et al. 2020)	Ø	↓ Δ, θ Ø α, γ	-
Dextromethorphan (non-competitive)	current study	Ø	↑ γ Ø Δ, θ, α, β	Ø all frequencies (single-pulse TMS) ↑ N45 (single-pulse TMS)

- incompatible method or not tested, ↑ increase or ↓ decrease or tested frequency, Ø no statistically measurable changes. Δ delta-band, θ theta-band, α alpha-band, β beta-band, γ gamma-band.

4.1.3 Reduced pre-enhanced cortical excitability by VGCC-antagonist

In spite of excitatory synaptic signaling by glutamate, rapid release of excitatory neurotransmitters underlies the regulatory mechanism of calcium channels (Dolphin and Lee 2020), but how VGCC contributes to cortico-cortical and cortico-spinal excitability has yet been less investigated. 30-40% of total electric current is driven by activation of L-type VGCC during synaptic transmissions between pyramidal neurons (Morton et al. 2013). However, pre-synaptic L-VGCC-activity is not substantially involved in the control of the release of glutamate during excitatory neurotransmission (Wankerl et al. 2010, Catterall 2011). Since limiting of postsynaptic calcium concentration can induce long-term-depression (Wankerl et al. 2010), and other types of VGCC (N and P/Q-type) did not relevantly affect cortico-cortical excitability (Heidegger 2010), postsynaptic L-type VGCC should play an important role in the regulatory system of calcium-related neuronal activation. In this study, nimodipine is used to inhibit post-synaptic L-type VGCC to investigate its role in corticospinal and synaptic excitability. In accordance with related studies (Wankerl et al. 2010, Weise et al. 2017), as shown in Table 5, no change of RMT or TEP has been observed (König et al. 2019), whereas power of gamma- and beta-oscillations increased after application of nimodipine in the resting-state EEG. So far, in-vivo resting-state EEG-changes on healthy human subjects after application of nimodipine have not been tested. (Herning et al. 1995) monitored EEG-changes on substance abusers after application of nimodipine and found an effect of increased alpha-oscillations, but without including gamma-oscillations into their analysis. However, the comparison to their results is limited since pre-existing EEG abnormalities, such as excessive EEG beta-activity (Herning et al. 1997) and reduced alpha-activities (King et al. 2000), can be found in chronic cocaine abusers. A similar increase of power of gamma-oscillations like in our study was found in an in-vitro study using nimodipine (Lu et al. 2011). The question of why single-pulse TMS did not affect induced and evoked EEG-responses after application of nimodipine can probably be explained by the observation that nimodipine only alters LTP-like plasticity, but not excitability per se. This conclusion was supported by earlier studies, in which the authors proved

a suppression of LTP-like plasticity by theta-burst stimulation (Wankerl et al. 2010) or PAS (Weise et al. 2017) after intake of nimodipine.

Table 5. Cortical responses to L-type VGCC-antagonists using different methods.

Used drug	Author	RMT	Resting-state oscillations	Main outcome after event trigger/ stimulation type or protocol
Nimodipine	(Deutz et al. 1986)	-	↓ Δ, θ, α, β	(in-vivo on rat brain)
Nimodipine	(Herning et al. 1995)		γ untested ↑ α Ø Δ, θ, β	on substance abusers
Nimodipine	(Wolters et al. 2003)			↓ decreased induced excitability by paired associative stimulation (PAS10)
Nimodipine	(Wankerl et al. 2010)	Ø	-	↓ decreased induced enhancement of cortico-spinal excitability by theta-burst stimulation (cTBS)
Nimodipine	(Lu et al. 2011)	-	↑ γ	(in-vitro on CA3 hippocampal neurons)
Nimodipine	(Weise et al. 2017)	Ø	-	Ø input-output curves (single pulse TMS) ↓ decreased induced enhancement of cortico spinal excitability by paired associative stimulation (PAS25)
Nimodipine	current study	↑	↑ γ, β Ø Δ, θ, α	Ø all frequencies (single-pulse TMS) Ø TEP

- incompatible method or not tested, ↑ increase, ↓ decrease, Ø no significant changes. Δ deta-band, θ theta-band, α alpha-band, β beta-band, γ gamma-band. To note: the significant beta-increase (p=0.03) in our study is probably less validated comparing to the gamma-increase (p=0.002).

4.2 TMS-induced oscillations

While we found remarkable post- to pre- drug differences in the resting-state EEG after perampanel and dextromethorphan, it is not clear why no significant TMS-induced spectral changes have been observed. One might speculate that in the presence of ionotropic glutamate antagonists, TMS induces an enhanced effect of transient phase resetting (Kawasaki et al. 2014). Such a phase-reset might flatten spectral distinction but boost phase-locked amplitudes of evoked cortical responses. Just as previously reported, perampanel reduces P70 and dextromethorphan increases N45 of TEP (König et al. 2019).

In addition, in the case of perampanel the dosage had to be lowered from 12 mg to 6 mg due to major adverse events, as discussed above. The reduced dosage of perampanel may be insufficient to suppress brain oscillations after each excitatory trigger by TMS at an intensity of 100% RMT, but it is sufficient for the cortical suppression without the TMS-trigger. Similarly, the dosage of dextromethorphan 120 mg may have been too little to produce measurable changes of TMS-induced EEG-oscillations.

But, alas, the effect of perampanel on TMS-EEG has never been examined so far, while only few studies investigated the impact of dextromethorphan on TMS-EEG recordings. In these studies, using LICI protocols (Salavati et al. 2018b) and single-pulse TMS (Hui et al. 2020), there were also no significant changes after application of dextromethorphan 150mg on LICI and TMS-evoked interhemispheric signal propagation (ISP). However, PAS-induced long-term potentiation (LTP) was found decreased by applying paired associative stimulation (PAS) under the influence of dextromethorphan 150mg (Salavati et al. 2018a). While spectral change of brain response can be clearly monitored by EEG during resting-state, it remains an open question whether a higher drug dosage can alter TMS-induced oscillatory EEG-responses. These questions warrant further investigation.

5 Summary

Pharmaco-TMS-EEG is a promising technique to investigate and modulate brain activity. This study explores cortical and corticospinal excitability via TMS-induced oscillatory EEG-responses by modifying synaptic glutamatergic and voltage-gated transmission, which is represented by AMPAR, NMDAR, and VGCC, respectively. Sixteen healthy male subjects completed the study with four sessions in a pseudo-randomized, placebo-controlled, double-blinded crossover study. EEG signals were recorded and analyzed by using 64 TMS-compatible electrode-channels at resting-state and when single TMS pulses were applied over the left primary motor cortex. Perampanel as the glutamatergic antagonist at AMPARs, dextromethorphan at NMDARs and nimodipine as the antagonist at L-type VGCC were used as negative modulators. It was found that perampanel and dextromethorphan have differential effects on resting-state EEG and TMS induced EEG-oscillations. Perampanel significantly increased RMT and power of all tested frequencies (Δ, θ, α and β) except for the fast γ-frequencies at resting-state. Dextromethorphan had no effect on RMT and lower frequencies but increased power of resting-state γ-oscillations. This highlights that the main mechanisms of AMPAR- and NMDAR-related glutamatergic transmission have different effects on cortical excitability. Nimodipine produced a similar effect on resting-state EEG to that yielded by dextromethorphan. It significantly increased power of resting-state γ- and β-oscillations. Although statistical change of power of TMS-induced oscillations has not been significantly observed under any of the tested drugs, amplitudes of TMS-evoked potentials were significantly changed, which was reflected particularly by a decreased P70 after perampanel and increased N45 after dextromethorphan intake (König et al. 2019). This may be explained by an effect of phase-resetting by TMS in the global excitatory system. There were no TMS-evoked or -induced effects under influence of nimodipine, consistently with the conclusion of previous studies that antagonizing neuronal VGCCs probably can only decrease pre-enhanced cortical excitability. It is expected that the obtained results can contribute to the understanding of excitability mechanisms of cortical excitatory networks in further studies.

6 Zusammenfassung

Pharmaco-TMS-EEG ist eine vielversprechende kombinierte Technik zur Modulation und Untersuchung von Hirnaktivitäten. Diese Studie erforscht die kortikale und kortikospinale Erregbarkeit anhand TMS-induzierter EEG-Signale, welche durch glutamaterge und spannungskontrollierte Neurotransmission der Synapsen hervorgerufen werden, die ihrerseits durch AMPA-, NMDA- und VGCC-Rezeptoren repräsentiert werden. Sechzehn gesunde männliche Probanden nahmen an der pseudo-randomisierten, doppel-verblindeten und Placebo-kontrollierten Studie teil. EEG-Signale wurden dabei mittels 64 TMS-kompatiblen Elektroden sowohl im Ruhezustand als auch während der Stimulationsphase des primären Motorcortex durch TMS-Einzelpulse aufgenommen und analysiert. Als negative Modulatoren wurden Perampanel, ein AMPA-Rezeptorantagonist, Dextromethorphan, ein NMDA-Rezeptorantagonist, und Nimodipin, ein VGCC-Antagonist hierbei eingesetzt. Wir konnten zeigen, dass verschiedene Glutamat-Rezeptorantagonisten zu spezifischen Veränderungen im Ruhe-EEG und im TMS-evozierten EEG führen. Perampanel konnte signifikant die motorische Reizschwelle und die Power in allen getesteten Frequenzbändern bis auf die γ-Frequenz im Ruhe-EEG erhöhen. Dextromethorphan wiederum hatte keinen Effekt auf die motorische Reizschwelle, konnte aber signifikant die Power im γ-Frequenzband im Ruhe-EEG erhöhen. Diese Ergebnisse betonen in erster Linie, dass der Mechanismus der AMPAR- und NMDAR-abhängigen Neurotransmission die kortikale Erregbarkeit unterschiedlich beeinflussen kann. Nimodipin hatte vergleichbare Effekte wie Dextromethorphan und steigerte signifikant die Stärke in den den ß- und γ-Frequenzbändern im Ruhe-EEG. Obwohl sich keine Änderungen der Frequenzstärken im TMS-induzierten EEG zeigten, wurden TMS-evozierte EEG-Amplituden durch Einfluss der Studienmedikamente signifikant verändert. Insbesondere wurde eine signifikante Senkung des P70 durch Perampanel und eine Steigerung des N45 durch Dextromethorphan ausgelöst (König et al. 2019). Dies könnte durch eine Phasenkorrektur im exzitatorischen System durch TMS erklärt werden. Unter Nimodipin konnte weder eine evozierte noch eine induzierte EEG-Signaländerung nach TMS-Stimulation beobachtet werden, was wiederum

früheren Beobachtungen entspricht, dass die Hemmung von VGCC wahrscheinlich nur eine Senkung einer vorher gesteigerte kortikale Exzitabilität bewirken kann. Diese Ergebnisse tragen zum besseren Verständnis kortikaler exzitatorischer Mechanismen bei und sollten in zukünftigen Studien weiter untersucht werden.

References

Artola, A., T. Hensch and W. Singer (1996). "Calcium-induced long-term depression in the visual cortex of the rat in vitro." Journal of Neurophysiology **76**(2): 984-994.

Aserinsky, E. and N. Kleitman (1953). "Regularly occurring periods of eye motility, and concomitant phenomena, during sleep." Science **118**(3062): 273-274.

Asztély, F. and B. Gustafsson (1996). "Ionotropic glutamate receptors." Molecular Neurobiology **12**(1): 1.

Babadi, B. and E. N. Brown (2014). "A Review of Multitaper Spectral Analysis." IEEE Transactions on Biomedical Engineering **61**(5): 1555-1564.

Barker, A. T., R. Jalinous and I. L. Freeston (1985). "Non-invasive magnetic stimulation of human motor cortex." Lancet **1**(8437): 1106-1107.

Barr, M. S., F. Farzan, K. D. Davis, P. B. Fitzgerald and Z. J. Daskalakis (2013). "Measuring GABAergic Inhibitory Activity with TMS-EEG and Its Potential Clinical Application for Chronic Pain." Journal of Neuroimmune Pharmacology **8**(3): 535-546.

Barygin, O. I. (2016). "Inhibition of calcium-permeable and calcium-impermeable AMPA receptors by perampanel in rat brain neurons." Neurosci Lett **633**: 146-151.

Baude, A., Z. Nusser, J. D. B. Roberts, E. Mulvihill, R. A. Jeffrey McIlhinney and P. Somogyi (1993). "The metabotropic glutamate receptor (mGluRIα) is concentrated at perisynaptic membrane of neuronal subpopulations as detected by immunogold reaction." Neuron **11**(4): 771-787.

Bean, B. P. (2007). "The action potential in mammalian central neurons." Nat Rev Neurosci **8**(6): 451-465.

Berger, H. (1929). "Über das Elektrenkephalogramm des Menschen." Archiv für Psychiatrie und Nervenkrankheiten **87**(1): 527-570.

Brady, S., G. Siegel, R. W. Albers and D. Price (2011). Basic Neurochemistry: Principles of Molecular, Cellular, and Medical Neurobiology, Elsevier Science.

Burnashev, N., A. Khodorova, P. Jonas, P. J. Helm, W. Wisden, H. Monyer, P. H. Seeburg and B. Sakmann (1992). "Calcium-permeable AMPA-kainate receptors in fusiform cerebellar glial cells." Science **256**(5063): 1566-1570.

Canali, P., S. Casarotto, M. Rosanova, G. Sferrazza-Papa, A. G. Casali, O. Gosseries, M. Massimini, E. Smeraldi, C. Colombo and F. Benedetti (2017). "Abnormal brain oscillations persist after recovery from bipolar depression." European Psychiatry **41**: 10-15.

Capon, D. A., F. Bochner, N. Kerry, G. Mikus, C. Danz and A. A. Somogyi (1996). "The influence of CYP2D6 polymorphism and quinidine on the

disposition and antitussive effect of dextromethorphan in humans." Clin Pharmacol Ther **60**(3): 295-307.

Carlson, C. and O. Devinsky (2009). "The excitable cerebral cortex Fritsch G, Hitzig E. Uber die elektrische Erregbarkeit des Grosshirns. Arch Anat Physiol Wissen 1870;37:300-32." Epilepsy Behav **15**(2): 131-132.

Casula, E. P., V. Tarantino, D. Basso, G. Arcara, G. Marino, G. M. Toffolo, J. C. Rothwell and P. S. Bisiacchi (2014). "Low-frequency rTMS inhibitory effects in the primary motor cortex: Insights from TMS-evoked potentials." NeuroImage **98**: 225-232.

Caton, R. (1875). "Electrical Currents of the Brain." The Journal of Nervous and Mental Disease **2**(4).

Catterall, W. A. (2011). "Voltage-gated calcium channels." Cold Spring Harb Perspect Biol **3**(8): a003947.

Catterall, W. A. and J. Striessnig (1992). "Receptor sites for Ca2+ channel antagonists." Trends Pharmacol Sci **13**(6): 256-262.

Chatterton, J. E., M. Awobuluyi, L. S. Premkumar, H. Takahashi, M. Talantova, Y. Shin, J. Cui, S. Tu, K. A. Sevarino, N. Nakanishi, G. Tong, S. A. Lipton and D. Zhang (2002). "Excitatory glycine receptors containing the NR3 family of NMDA receptor subunits." Nature **415**(6873): 793-798.

Cherubini, E., M. Griguoli, V. Safiulina and L. Lagostena (2011). "The depolarizing action of GABA controls early network activity in the developing hippocampus." Mol Neurobiol **43**(2): 97-106.

Chrobak, J. and G. Buzsáki (1998). "Gamma Oscillations in the Entorhinal Cortex of the Freely Behaving Rat." The Journal of neuroscience : the official journal of the Society for Neuroscience **18**: 388-398.

Chung, S. W., A. T. Hill, N. C. Rogasch, K. E. Hoy and P. B. Fitzgerald (2016). "Use of theta-burst stimulation in changing excitability of motor cortex: A systematic review and meta-analysis." Neuroscience & Biobehavioral Reviews **63**: 43-64.

Chung, S. W., N. C. Rogasch, K. E. Hoy and P. B. Fitzgerald (2015). "Measuring Brain Stimulation Induced Changes in Cortical Properties Using TMS-EEG." Brain Stimul **8**(6): 1010-1020.

Church, J., D. Lodge and S. C. Berry (1985). "Differential effects of dextrorphan and levorphanol on the excitation of rat spinal neurons by amino acids." Eur J Pharmacol **111**(2): 185-190.

Cichy, R. M. and D. Pantazis (2017). "Multivariate pattern analysis of MEG and EEG: A comparison of representational structure in time and space." Neuroimage **158**: 441-454.

Clements, J. D., A. Feltz, Y. Sahara and G. L. Westbrook (1998). "Activation Kinetics of AMPA Receptor Channels Reveal the Number of Functional Agonist Binding Sites." The Journal of Neuroscience **18**(1): 119-127.

Clements, J. D. and G. L. Westbrook (1991). "Activation kinetics reveal the number of glutamate and glycine binding sites on the N-methyl-D-aspartate receptor." Neuron **7**(4): 605-613.

Cohen, M. X. (2019). "A better way to define and describe Morlet wavelets for time-frequency analysis." NeuroImage **199**: 81-86.

Collingridge, G. L. and T. V. P. Bliss (1995). "Memories of NMDA receptors and LTP." Trends in Neurosciences **18**(2): 54-56.

Conn, P. J. (2003). "Physiological roles and therapeutic potential of metabotropic glutamate receptors." Ann N Y Acad Sci **1003**: 12-21.

Contractor, A., C. Mulle and G. T. Swanson (2011). "Kainate receptors coming of age: milestones of two decades of research." Trends Neurosci **34**(3): 154-163.

Cracco, R. Q., V. E. Amassian, P. J. Maccabee and J. B. Cracco (1989). "Comparison of human transcallosal responses evoked by magnetic coil and electrical stimulation." Electroencephalogr Clin Neurophysiol **74**(6): 417-424.

Darmani, G., C. M. Zipser, G. M. Böhmer, K. Deschet, F. Müller-Dahlhaus, P. Belardinelli, M. Schwab and U. Ziemann (2016). "Effects of the Selective α5-GABAAR Antagonist S44819 on Excitability in the Human Brain: A TMS-EMG and TMS-EEG Phase I Study." J Neurosci **36**(49): 12312-12320.

Daskalakis, Z. J., B. K. Christensen, P. B. Fitzgerald, L. Roshan and R. Chen (2002). "The mechanisms of interhemispheric inhibition in the human motor cortex." J Physiol **543**(Pt 1): 317-326.

Daskalakis, Z. J., F. Farzan, M. S. Barr, J. J. Maller, R. Chen and P. B. Fitzgerald (2008). "Long-Interval Cortical Inhibition from the Dorsolateral Prefrontal Cortex: a TMS–EEG Study." Neuropsychopharmacology **33**(12): 2860-2869.

Daskalakis, Z. J., F. Farzan, N. Radhu and P. B. Fitzgerald (2012). "Combined transcranial magnetic stimulation and electroencephalography: its past, present and future." Brain Res **1463**: 93-107.

Daskalakis, Z. J., F. Farzan, N. Radhu and P. B. Fitzgerald (2012). "Combined transcranial magnetic stimulation and electroencephalography: Its past, present and future." Brain Research **1463**: 93-107.

de Leon, J., M. T. Susce, R. M. Pan, M. Fairchild, W. H. Koch and P. J. Wedlund (2005). "The CYP2D6 poor metabolizer phenotype may be associated with risperidone adverse drug reactions and discontinuation." J Clin Psychiatry **66**(1): 15-27.

Deng, Z. D., S. H. Lisanby and A. V. Peterchev (2014). "Coil design considerations for deep transcranial magnetic stimulation." Clin Neurophysiol **125**(6): 1202-1212.

Deutz, N. E., R. A. Chamuleau, W. M. Bovée and A. J. Van der Werf (1986). "Effects of nimodipine on EEG and 31P-NMR spectra during and after incomplete forebrain ischemia in the rat." European journal of pharmacology **125**(3): 429-435.

Di Lazzaro, V. and U. Ziemann (2013). "The contribution of transcranial magnetic stimulation in the functional evaluation of microcircuits in human motor cortex." Frontiers in neural circuits **7**: 18-18.

Diering, G. H. and R. L. Huganir (2018). "The AMPA Receptor Code of Synaptic Plasticity." Neuron **100**(2): 314-329.

Dolphin, A. C. and A. Lee (2020). "Presynaptic calcium channels: specialized control of synaptic neurotransmitter release." Nat Rev Neurosci **21**(4): 213-229.

Dutra, T. G., A. Baltar and K. K. Monte-Silva (2016). "Motor cortex excitability in attention-deficit hyperactivity disorder (ADHD): A systematic review and meta-analysis." Research in Developmental Disabilities **56**: 1-9.

Dzamba, D., P. Honsa and M. Anderova (2013). "NMDA Receptors in Glial Cells: Pending Questions." Current neuropharmacology **11**(3): 250-262.

Engel, A. K. and P. Fries (2010). "Beta-band oscillations—signalling the status quo?" Current Opinion in Neurobiology **20**(2): 156-165.

Engel, A. K. and W. Singer (2001). "Temporal binding and the neural correlates of sensory awareness." Trends in Cognitive Sciences **5**(1): 16-25.

Epstein, C. M., E. M. Wassermann and U. Ziemann (2012). Oxford Handbook of Transcranial Stimulation, Oxford University Press.

Esser, S. K., R. Huber, M. Massimini, M. J. Peterson, F. Ferrarelli and G. Tononi (2006). "A direct demonstration of cortical LTP in humans: A combined TMS/EEG study." Brain Research Bulletin **69**(1): 86-94.

Farzan, F., M. Vernet, M. M. D. Shafi, A. Rotenberg, Z. J. Daskalakis and A. Pascual-Leone (2016). "Characterizing and Modulating Brain Circuitry through Transcranial Magnetic Stimulation Combined with Electroencephalography." Frontiers in Neural Circuits **10**(73).

Ferreri, F., P. Pasqualetti, S. Määttä, D. Ponzo, F. Ferrarelli, G. Tononi, E. Mervaala, C. Miniussi and P. M. Rossini (2011). "Human brain connectivity during single and paired pulse transcranial magnetic stimulation." Neuroimage **54**(1): 90-102.

Ferreri, F., F. Vecchio, L. Vollero, A. Guerra, S. Petrichella, D. Ponzo, S. Määtta, E. Mervaala, M. Könönen, F. Ursini, P. Pasqualetti, G. Iannello, P. M. Rossini and V. Di Lazzaro (2016). "Sensorimotor cortex excitability and connectivity in Alzheimer's disease: A TMS-EEG Co-registration study." Human Brain Mapping **37**(6): 2083-2096.

Franco, V., F. Crema, A. Iudice, G. Zaccara and E. Grillo (2013). "Novel treatment options for epilepsy: Focus on perampanel." Pharmacological Research **70**(1): 35-40.

Freche, D., J. Naim-Feil, A. Peled, N. Levit-Binnun and E. Moses (2018). "A quantitative physical model of the TMS-induced discharge artifacts in EEG." PLoS computational biology **14**(7): e1006177-e1006177.

Fuchs, E. C., H. Doheny, H. Faulkner, A. Caputi, R. D. Traub, A. Bibbig, N. Kopell, M. A. Whittington and H. Monyer (2001). "Genetically altered AMPA-type glutamate receptor kinetics in interneurons disrupt long-range synchrony of gamma oscillation." Proceedings of the National Academy of Sciences **98**(6): 3571-3576.

Fuggetta, G., A. Fiaschi and P. Manganotti (2005). "Modulation of cortical oscillatory activities induced by varying single-pulse transcranial magnetic stimulation intensity over the left primary motor area: A combined EEG and TMS study." NeuroImage **27**(4): 896-908.

Furukawa, H. (2012). "Structure and function of glutamate receptor amino terminal domains." The Journal of Physiology **590**(1): 63-72.

Geddes, L. A. (1991). "History of magnetic stimulation of the nervous system." J Clin Neurophysiol **8**(1): 3-9.

Gibbs, F. A., H. Davis and W. G. Lennox (1935). "THE ELECTRO-ENCEPHALOGRAM IN EPILEPSY AND IN CONDITIONS OF IMPAIRED CONSCIOUSNESS." Archives of Neurology & Psychiatry **34**(6): 1133-1148.

Gidal, B. E., R. Maganti, A. Laurenza, H. Yang, D. A. Verbel, E. Schuck and J. Ferry (2017). "Effect of enzyme inhibition on perampanel pharmacokinetics: Why study design matters." Epilepsy Research **134**: 41-48.

Gordon, E. (2003). Integrative Neuroscience: Bringing Together Biological, Psychological and Clinical Models of the Human Brain, Taylor & Francis.

Groppa, S., A. Oliviero, A. Eisen, A. Quartarone, L. G. Cohen, V. Mall, A. Kaelin-Lang, T. Mima, S. Rossi, G. W. Thickbroom, P. M. Rossini, U. Ziemann, J. Valls-Solé and H. R. Siebner (2012). "A practical guide to diagnostic transcranial magnetic stimulation: report of an IFCN committee." Clin Neurophysiol **123**(5): 858-882.

Gutierrez-Castellanos, N., C. M. Da Silva-Matos, K. Zhou, C. B. Canto, M. C. Renner, L. M. C. Koene, O. Ozyildirim, R. Sprengel, H. W. Kessels and C. I. De Zeeuw (2017). "Motor Learning Requires Purkinje Cell Synaptic Potentiation through Activation of AMPA-Receptor Subunit GluA3." Neuron **93**(2): 409-424.

Hakami, T., N. C. Jones, E. A. Tolmacheva, J. Gaudias, J. Chaumont, M. Salzberg, T. J. O'Brien and D. Pinault (2009). "NMDA Receptor Hypofunction Leads to Generalized and Persistent Aberrant γ Oscillations Independent of Hyperlocomotion and the State of Consciousness." PLOS ONE **4**(8): e6755.

Hallett, M. (2007). "Transcranial Magnetic Stimulation: A Primer." Neuron **55**(2): 187-199.

Hammond, C. (2015). Chapter 10 - The ionotropic glutamate receptors. Cellular and Molecular Neurophysiology (Fourth Edition). C. Hammond. Boston, Academic Press**:** 221-244.

Hanley, M. J., P. Cancalon, W. W. Widmer and D. J. Greenblatt (2011). "The effect of grapefruit juice on drug disposition." Expert opinion on drug metabolism & toxicology **7**(3): 267-286.

Herning, R. I., X. Guo, W. E. Better, L. L. Weinhold, W. R. Lange, J. L. Cadet and D. A. Gorelick (1997). "Neurophysiological signs of cocaine dependence: Increased electroencephalogram beta during withdrawal." Biological Psychiatry **41**(11): 1087-1094.

Herning, R. I., X. Guo and W. R. Lange (1995). "The effects of nimodipine on the EEG of substance abusers." Ann N Y Acad Sci **765**: 143-151; discussion 160-142.

Herring, B. E. and R. A. Nicoll (2016). "Long-Term Potentiation: From CaMKII to AMPA Receptor Trafficking." Annu Rev Physiol **78**: 351-365.

Herring, J. D., G. Thut, O. Jensen and T. O. Bergmann (2015). "Attention Modulates TMS-Locked Alpha Oscillations in the Visual Cortex." The Journal of Neuroscience **35**(43): 14435.

Herrmann, C. S., S. Rach, J. Vosskuhl and D. Strüber (2014). "Time-frequency analysis of event-related potentials: a brief tutorial." Brain Topogr **27**(4): 438-450.

Herrmann, C. S., D. Senkowski and S. Röttger (2004). "Phase-locking and amplitude modulations of EEG alpha: Two measures reflect different cognitive processes in a working memory task." Exp Psychol **51**(4): 311-318.

Hill, A. T., N. C. Rogasch, P. B. Fitzgerald and K. E. Hoy (2016). "TMS-EEG: A window into the neurophysiological effects of transcranial electrical stimulation in non-motor brain regions." Neuroscience & Biobehavioral Reviews **64**: 175-184.

Huganir, R. L. and R. A. Nicoll (2013). "AMPARs and synaptic plasticity: the last 25 years." Neuron **80**(3): 704-717.

Hui, J., R. Zomorrodi, P. Lioumis, B. Salavati, T. K. Rajji, R. Chen, D. M. Blumberger and Z. J. Daskalakis (2020). "Pharmacological mechanisms of interhemispheric signal propagation: a TMS-EEG study." Neuropsychopharmacology **45**(6): 932-939.

Hutchison, I. C. and S. Rathore (2015). "The role of REM sleep theta activity in emotional memory." Frontiers in psychology **6**: 1439-1439.

Huxley, A. F. (2002). "Hodgkin and the action potential 1935-1952." J Physiol **538**(Pt 1): 2.

Igelmund, P., Y. Q. Zhao and U. Heinemann (1996). "Effects of T-type, L-type, N-type, P-type, and Q-type calcium channel blockers on stimulus-induced pre- and postsynaptic calcium fluxes in rat hippocampal slices." Exp Brain Res **109**(1): 22-32.

Ilmoniemi, R. J. and D. Kičić (2009). "Methodology for Combined TMS and EEG." Brain Topography **22**(4): 233.

Ilmoniemi, R. J., J. Virtanen, J. Ruohonen, J. Karhu, H. J. Aronen, R. Näätänen and T. Katila (1997). "Neuronal responses to magnetic stimulation reveal cortical reactivity and connectivity." NeuroReport **8**(16): 3537-3540.

Ilmoniemi, R. J., J. Virtanen, J. Ruohonen, J. Karhu, H. J. Aronen, R. Näätänen and T. Katila (1997). "Neuronal responses to magnetic stimulation reveal cortical reactivity and connectivity." Neuroreport **8**(16): 3537-3540.

Ishii, T., K. Moriyoshi, H. Sugihara, K. Sakurada, H. Kadotani, M. Yokoi, C. Akazawa, R. Shigemoto, N. Mizuno, M. Masu and et al. (1993). "Molecular characterization of the family of the N-methyl-D-aspartate receptor subunits." J Biol Chem **268**(4): 2836-2843.

Jang, H. J., K. Park, J. Lee, H. Kim, K. H. Han and J. Kwag (2015). "GABAA receptor-mediated feedforward and feedback inhibition differentially modulate the gain and the neural code transformation in hippocampal CA1 pyramidal cells." Neuropharmacology **99**: 177-186.

Jensen, O., P. Goel, N. Kopell, M. Pohja, R. Hari and B. Ermentrout (2005). "On the human sensorimotor-cortex beta rhythm: Sources and modeling." NeuroImage **26**(2): 347-355.

Jensen, O., E. Spaak and J. Zumer (2014). Human Brain Oscillations: From Physiological Mechanisms to Analysis and Cognition**:** 359-404.

Johnson, N. W., M. Özkan, A. P. Burgess, E. J. Prokic, K. A. Wafford, M. J. O'Neill, S. D. Greenhill, I. M. Stanford and G. L. Woodhall (2017). "Phase-amplitude coupled persistent theta and gamma oscillations in rat primary motor cortex in vitro." Neuropharmacology **119**: 141-156.

Jonas, P., C. Racca, B. Sakmann, P. H. Seeburg and H. Monyer (1994). "Differences in Ca2+ permeability of AMPA-type glutamate receptor channels in neocortical neurons caused by differential GluR-B subunit expression." Neuron **12**(6): 1281-1289.

Jordan, K. G. (1999). "Continuous EEG Monitoring in the Neuroscience Intensive Care Unit and Emergency Department." Journal of Clinical Neurophysiology **16**(1): 14-39.

Julkunen, P., A. Pääkkönen, T. Hukkanen, M. Könönen, P. Tiihonen, S. Vanhatalo and J. Karhu (2008). "Efficient reduction of stimulus artefact in TMS–EEG by epithelial short-circuiting by mini-punctures." Clinical Neurophysiology **119**(2): 475-481.

Kammer, T., S. Beck, M. Erb and W. Grodd (2001). "The influence of current direction on phosphene thresholds evoked by transcranial magnetic stimulation." Clin Neurophysiol **112**(11): 2015-2021.

Kammer, T., S. Beck, A. Thielscher, U. Laubis-Herrmann and H. Topka (2001). "Motor thresholds in humans: a transcranial magnetic stimulation study comparing different pulse waveforms, current directions and stimulator types." Clinical Neurophysiology **112**(2): 250-258.

Kawasaki, M., Y. Uno, J. Mori, K. Kobata and K. Kitajo (2014). "Transcranial magnetic stimulation-induced global propagation of transient

phase resetting associated with directional information flow." Frontiers in human neuroscience **8**: 173-173.

King, D. E., R. I. Herning, D. A. Gorelick and J. L. Cadet (2000). "Gender Differences in the EEG of Abstinent Cocaine Abusers." Neuropsychobiology **42**(2): 93-98.

Kirschfeld, K. (2009). "The modulation of alpha-wave amplitude in human EEG by the intention to act with a motor response." Nature Precedings.

Kirschstein, T. and R. Köhling (2009). "What is the source of the EEG?" Clin EEG Neurosci **40**(3): 146-149.

Klamer, S., A. Elshahabi, H. Lerche, C. Braun, M. Erb, K. Scheffler and N. K. Focke (2015). "Differences between MEG and high-density EEG source localizations using a distributed source model in comparison to fMRI." Brain Topogr **28**(1): 87-94.

Knyazev, G. G. (2012). "EEG delta oscillations as a correlate of basic homeostatic and motivational processes." Neuroscience & Biobehavioral Reviews **36**(1): 677-695.

Komssi, S. and S. Kähkönen (2006). "The novelty value of the combined use of electroencephalography and transcranial magnetic stimulation for neuroscience research." Brain Research Reviews **52**(1): 183-192.

Komssi, S., S. Kähkönen and R. J. Ilmoniemi (2004). "The effect of stimulus intensity on brain responses evoked by transcranial magnetic stimulation." Hum Brain Mapp **21**(3): 154-164.

König, F., P. Belardinelli, C. Liang, D. Desideri, F. Müller-Dahlhaus, P. C. Gordon, C. Zipser, C. Zrenner and U. Ziemann (2019). "TMS-EEG signatures of glutamatergic neurotransmission in human cortex." bioRxiv: 555920. (only available online)

Korotkova, T., E. C. Fuchs, A. Ponomarenko, J. von Engelhardt and H. Monyer (2010). "NMDA Receptor Ablation on Parvalbumin-Positive Interneurons Impairs Hippocampal Synchrony, Spatial Representations, and Working Memory." Neuron **68**(3): 557-569.

Krauss, G. L., E. Perucca, E. Ben-Menachem, P. Kwan, J. J. Shih, D. Squillacote, H. Yang, M. Gee, J. Zhu and A. Laurenza (2013). "Perampanel, a selective, noncompetitive α-amino-3-hydroxy-5-methyl-4-isoxazolepropionic acid receptor antagonist, as adjunctive therapy for refractory partial-onset seizures: interim results from phase III, extension study 307." Epilepsia **54**(1): 126-134.

Krieg, S. M. (2017). Navigated Transcranial Magnetic Stimulation in Neurosurgery, Springer International Publishing.

Kriz, J., G. Zupan and A. Simonić (2003). "Differential effects of dihydropyridine calcium channel blockers in kainic acid-induced experimental seizures in rats." Epilepsy Res **52**(3): 215-225.

Kuczewski, N., C. Porcher and J. L. Gaiarsa (2010). "Activity-dependent dendritic secretion of brain-derived neurotrophic factor modulates synaptic plasticity." Eur J Neurosci **32**(8): 1239-1244.

Kwiecien, R. and C. Hammond (1998). "Differential management of Ca2+ oscillations by anterior pituitary cells: a comparative overview." Neuroendocrinology **68**(3): 135-151.

Kwiecien, R., C. Robert, R. Cannon, S. Vigues, A. Arnoux, C. Kordon and C. Hammond (1998). "Endogenous pacemaker activity of rat tumour somatotrophs." J Physiol **508 (Pt 3)**(Pt 3): 883-905.

Lee, L., L. M. Harrison and A. Mechelli (2003). "The Functional Brain Connectivity Workshop: report and commentary." Network **14**(2): R1-15.

Lester, R. A. J., J. D. Clements, G. L. Westbrook and C. E. Jahr (1990). "Channel kinetics determine the time course of NMDA receptor-mediated synaptic currents." Nature **346**(6284): 565-567.

Light, G. A., L. E. Williams, F. Minow, J. Sprock, A. Rissling, R. Sharp, N. R. Swerdlow and D. L. Braff (2010). "Electroencephalography (EEG) and event-related potentials (ERPs) with human participants." Current protocols in neuroscience **Chapter 6**: Unit-6.25.24.

Lipscombe, D., T. D. Helton and W. Xu (2004). "L-type calcium channels: the low down." J Neurophysiol **92**(5): 2633-2641.

Lu, C. B., J. B. Hamilton, A. D. Powell, E. C. Toescu and M. Vreugdenhil (2011). "Effect of ageing on CA3 interneuron sAHP and gamma oscillations is activity-dependent." Neurobiology of Aging **32**(5): 956-965.

Madsen, K. H., L. Ewald, H. R. Siebner and A. Thielscher (2015). "Transcranial Magnetic Stimulation: An Automated Procedure to Obtain Coil-specific Models for Field Calculations." Brain Stimulation **8**(6): 1205-1208.

Maris, E. and R. Oostenveld (2007). "Nonparametric statistical testing of EEG- and MEG-data." Journal of Neuroscience Methods **164**(1): 177-190.

Mayer, M. L., A. B. MacDermott, G. L. Westbrook, S. J. Smith and J. L. Barker (1987). "Agonist- and voltage-gated calcium entry in cultured mouse spinal cord neurons under voltage clamp measured using arsenazo III." J Neurosci **7**(10): 3230-3244.

McNally, J. M., R. W. McCarley, J. T. McKenna, Y. Yanagawa and R. E. Brown (2011). "Complex receptor mediation of acute ketamine application on in vitro gamma oscillations in mouse prefrontal cortex: modeling gamma band oscillation abnormalities in schizophrenia." Neuroscience **199**: 51-63.

Monsalve, I. F., M. Bourguignon and N. Molinaro (2018). "Theta oscillations mediate pre-activation of highly expected word initial phonemes." Scientific Reports **8**(1): 9503.

Morton, R. A., M. S. Norlin, C. C. Vollmer and C. F. Valenzuela (2013). "Characterization of L-type voltage-gated Ca(2+) channel expression and function in developing CA3 pyramidal neurons." Neuroscience **238**: 59-70.

Mueller, J. K., E. M. Grigsby, V. Prevosto, F. W. Petraglia, H. Rao, Z.-D. Deng, A. V. Peterchev, M. A. Sommer, T. Egner, M. L. Platt and W. M. Grill (2014). "Simultaneous transcranial magnetic stimulation and single-neuron recording in alert non-human primates." Nature Neuroscience **17**(8): 1130-1136.

Muthukumaraswamy, S. D. (2010). "Functional Properties of Human Primary Motor Cortex Gamma Oscillations." Journal of Neurophysiology **104**(5): 2873-2885.

Muthukumaraswamy, S. D., B. Routley, W. Droog, K. D. Singh and K. Hamandi (2016). "The effects of AMPA blockade on the spectral profile of human early visual cortex recordings studied with non-invasive MEG." Cortex **81**: 266-275.

Nakamura, H., H. Kitagawa, Y. Kawaguchi and H. Tsuji (1997). "Intracortical facilitation and inhibition after transcranial magnetic stimulation in conscious humans." J Physiol **498 (Pt 3)**(Pt 3): 817-823.

Neuper, C., R. H. Grabner, A. Fink and A. C. Neubauer (2005). "Long-term stability and consistency of EEG event-related (de-)synchronization across different cognitive tasks." Clinical Neurophysiology **116**(7): 1681-1694.

Nguyen, L., K. L. Thomas, B. P. Lucke-Wold, J. Z. Cavendish, M. S. Crowe and R. R. Matsumoto (2016). "Dextromethorphan: An update on its utility for neurological and neuropsychiatric disorders." Pharmacol Ther **159**: 1-22.

Nimmrich, V. and G. Gross (2012). "P/Q-type calcium channel modulators." British journal of pharmacology **167**(4): 741-759.

Nusser, Z., E. Mulvihill, P. Streit and P. Somogyi (1994). "Subsynaptic segregation of metabotropic and ionotropic glutamate receptors as revealed by immunogold localization." Neuroscience **61**(3): 421-427.

Oostenveld, R., P. Fries, E. Maris and J.-M. Schoffelen (2011). "FieldTrip: Open Source Software for Advanced Analysis of MEG, EEG, and Invasive Electrophysiological Data." Computational intelligence and neuroscience **2011**: 156869.

Pachernegg, S., N. Strutz-Seebohm and M. Hollmann (2012). "GluN3 subunit-containing NMDA receptors: not just one-trick ponies." Trends Neurosci **35**(4): 240-249.

Paffi, A., F. Camera, F. Carducci, G. Rubino, P. Tampieri, M. Liberti and F. Apollonio (2015). "A Computational Model for Real-Time Calculation of Electric Field due to Transcranial Magnetic Stimulation in Clinics." International Journal of Antennas and Propagation **2015**: 11.

Patsalos, P. N. (2015). "The clinical pharmacology profile of the new antiepileptic drug perampanel: A novel noncompetitive AMPA receptor antagonist." Epilepsia **56**(1): 12-27.

Paus, T., P. K. Sipila and A. P. Strafella (2001). "Synchronization of Neuronal Activity in the Human Primary Motor Cortex by Transcranial Magnetic Stimulation: An EEG Study." Journal of Neurophysiology **86**(4): 1983-1990.

Pawley, A. D., F. A. Chowdhury, C. Tangwiriyasakul, B. Ceronie, R. D. C. Elwes, L. Nashef and M. P. Richardson (2017). "Cortical excitability correlates with seizure control and epilepsy duration in chronic epilepsy." Annals of clinical and translational neurology **4**(2): 87-97.

Pelkey, Kenneth A., E. Barksdale, Michael T. Craig, X. Yuan, M. Sukumaran, Geoffrey A. Vargish, Robert M. Mitchell, Megan S. Wyeth, Ronald S. Petralia, R. Chittajallu, R.-M. Karlsson, Heather A. Cameron, Y. Murata, Matthew T. Colonnese, Paul F. Worley and Chris J. McBain (2015). "Pentraxins Coordinate Excitatory Synapse Maturation and Circuit Integration of Parvalbumin Interneurons." Neuron **85**(6): 1257-1272.

Pellicciari, M. C., D. Veniero and C. Miniussi (2017). "Characterizing the Cortical Oscillatory Response to TMS Pulse." Frontiers in cellular neuroscience **11**: 38-38.

Pernet, C. R., M. Latinus, T. E. Nichols and G. A. Rousselet (2015). "Cluster-based computational methods for mass univariate analyses of event-related brain potentials/fields: A simulation study." Journal of neuroscience methods **250**: 85-93.

Perrin, F., J. Pernier, O. Bertrand and J. F. Echallier (1989). "Spherical splines for scalp potential and current density mapping." Electroencephalography and Clinical Neurophysiology **72**(2): 184-187.

Petralia, R. S., Y. X. Wang, E. Mayat and R. J. Wenthold (1997). "Glutamate receptor subunit 2-selective antibody shows a differential distribution of calcium-impermeable AMPA receptors among populations of neurons." J Comp Neurol **385**(3): 456-476.

Petrov, P. I., S. Mandija, I. E. C. Sommer, C. A. T. van den Berg and S. F. W. Neggers (2017). "How much detail is needed in modeling a transcranial magnetic stimulation figure-8 coil: Measurements and brain simulations." PloS one **12**(6): e0178952-e0178952.

Pfaff, G., P. Briegel and I. Lamprecht (1983). "Inter-individual variation in the metabolism of dextromethorphan." International Journal of Pharmaceutics **14**(2): 173-189.

Philippon, J., R. Grob, F. Dagreou, M. Guggiari, M. Rivierez and P. Viars (1986). "Prevention of vasospasm in subarachnoid haemorrhage. A controlled study with nimodipine." Acta Neurochir (Wien) **82**(3-4): 110-114.

Pinault, D. (2008). "N-Methyl d-Aspartate Receptor Antagonists Ketamine and MK-801 Induce Wake-Related Aberrant γ Oscillations in the Rat Neocortex." Biological Psychiatry **63**(8): 730-735.

Pinky, N. F., C. M. Wilkie, J. R. Barnes and M. P. Parsons (2018). "Region- and Activity-Dependent Regulation of Extracellular Glutamate." J Neurosci **38**(23): 5351-5366.

Polson, M. J., A. T. Barker and I. L. Freeston (1982). "Stimulation of nerve trunks with time-varying magnetic fields." Med Biol Eng Comput **20**(2): 243-244.

Premoli, I., T. O. Bergmann, M. Fecchio, M. Rosanova, A. Biondi, P. Belardinelli and U. Ziemann (2017). "The impact of GABAergic drugs on TMS-induced brain oscillations in human motor cortex." Neuroimage **163**: 1-12.

Premoli, I., N. Castellanos, D. Rivolta, P. Belardinelli, R. Bajo, C. Zipser, S. Espenhahn, T. Heidegger, F. Muller-Dahlhaus and U. Ziemann (2014). "TMS-EEG signatures of GABAergic neurotransmission in the human cortex." J Neurosci **34**(16): 5603-5612.

Premoli, I., J. Király, F. Müller-Dahlhaus, C. M. Zipser, P. Rossini, C. Zrenner, U. Ziemann and P. Belardinelli (2018). "Short-interval and long-interval intracortical inhibition of TMS-evoked EEG potentials." Brain Stimulation **11**(4): 818-827.

Premoli, I., J. Király, F. Müller-Dahlhaus, C. M. Zipser, P. Rossini, C. Zrenner, U. Ziemann and P. Belardinelli (2018). "Short-interval and long-interval intracortical inhibition of TMS-evoked EEG potentials." Brain Stimul **11**(4): 818-827.

R.C.Oldfield (1971). The assessment and analysis of handedness: The Edinburgh inventory. Edinburgh University, Scotland Neuropsychologia, 1971, Vol. 9, pp. 97 to 113. Pergamon Press. .

Radhu, N., L. N. Ravindran, A. J. Levinson and Z. J. Daskalakis (2012). "Inhibition of the cortex using transcranial magnetic stimulation in psychiatric populations: current and future directions." J Psychiatry Neurosci **37**(6): 369-378.

Reiner, A. and J. Levitz (2018). "Glutamatergic Signaling in the Central Nervous System: Ionotropic and Metabotropic Receptors in Concert." Neuron **98**(6): 1080-1098.

Renner, M. C., E. H. Albers, N. Gutierrez-Castellanos, N. R. Reinders, A. N. van Huijstee, H. Xiong, T. R. Lodder and H. W. Kessels (2017). "Synaptic plasticity through activation of GluA3-containing AMPA-receptors." Elife **6**.

Roach, B. J. and D. H. Mathalon (2008). "Event-Related EEG Time-Frequency Analysis: An Overview of Measures and An Analysis of Early Gamma Band Phase Locking in Schizophrenia." Schizophrenia Bulletin **34**(5): 907-926.

Roach, B. J. and D. H. Mathalon (2008). "Event-related EEG time-frequency analysis: an overview of measures and an analysis of early gamma band phase locking in schizophrenia." Schizophr Bull **34**(5): 907-926.

Rogasch, N. C., Z. J. Daskalakis and P. B. Fitzgerald (2013). "Cortical Inhibition, Excitation, and Connectivity in Schizophrenia: A Review of Insights From Transcranial Magnetic Stimulation." Schizophrenia Bulletin **40**(3): 685-696.

Rogasch, N. C., Z. J. Daskalakis and P. B. Fitzgerald (2015). "Cortical inhibition of distinct mechanisms in the dorsolateral prefrontal cortex is related to working memory performance: A TMS–EEG study." Cortex **64**: 68-77.

Rogasch, N. C. and P. B. Fitzgerald (2013). "Assessing cortical network properties using TMS-EEG." Hum Brain Mapp **34**(7): 1652-1669.

Rogasch, N. C., R. H. Thomson, F. Farzan, B. M. Fitzgibbon, N. W. Bailey, J. C. Hernandez-Pavon, Z. J. Daskalakis and P. B. Fitzgerald (2014). "Removing artefacts from TMS-EEG recordings using independent component analysis: importance for assessing prefrontal and motor cortex network properties." Neuroimage **101**: 425-439.

Rogasch, N. C., C. Zipser, G. Darmani, T. P. Mutanen, M. Biabani, C. Zrenner, D. Desideri, P. Belardinelli, F. Müller-Dahlhaus and U. Ziemann (2019). "TMS-evoked EEG potentials from prefrontal and parietal cortex: reliability, site specificity, and effects of NMDA receptor blockade." bioRxiv: 480111.

Rogasch, N. C., C. Zipser, G. Darmani, T. P. Mutanen, M. Biabani, C. Zrenner, D. Desideri, P. Belardinelli, F. Müller-Dahlhaus and U. Ziemann (2020). "The effects of NMDA receptor blockade on TMS-evoked EEG potentials from prefrontal and parietal cortex." Sci Rep **10**(1): 3168.

Rogawski, M. A. (2011). "Revisiting AMPA Receptors as an Antiepileptic Drug Target: Revisiting AMPA Receptors as an Antiepileptic Drug Target." Epilepsy Currents **11**(2): 56-63.

Rohracher, A., G. Zimmermann, V. Villanueva, I. Garamendi, J. W. Sander, T. Wehner, R. Shankar, E. Ben-Menachem, M. J. Brodie, M. C. Pensel, G. Di Gennaro, A. Maurousset, A. Strzelczyk, S. Rheims, A. Rácz, K. Menzler, V. Bertol-Alegre, I. García-Morales, F. J. López-González, M. Toledo, K. J. Carpenter and E. Trinka (2018). "Perampanel in routine clinical use across Europe: Pooled, multicenter, observational data." Epilepsia **59**(9): 1727-1739.

Rosanova, M., A. Casali, V. Bellina, F. Resta, M. Mariotti and M. Massimini (2009). "Natural frequencies of human corticothalamic circuits." J Neurosci **29**(24): 7679-7685.

Rossi, S., M. Hallett, P. M. Rossini and A. Pascual-Leone (2011). "Screening questionnaire before TMS: An update." Clinical Neurophysiology **122**(8): 1686.

Rossini, P. M., D. Burke, R. Chen, L. G. Cohen, Z. Daskalakis, R. Di Iorio, V. Di Lazzaro, F. Ferreri, P. B. Fitzgerald, M. S. George, M. Hallett, J. P. Lefaucheur, B. Langguth, H. Matsumoto, C. Miniussi, M. A. Nitsche, A. Pascual-Leone, W. Paulus, S. Rossi, J. C. Rothwell, H. R. Siebner, Y. Ugawa, V. Walsh and U. Ziemann (2015). "Non-invasive electrical and magnetic stimulation of the brain, spinal cord, roots and peripheral nerves: Basic principles and procedures for routine clinical and research application. An updated report from an I.F.C.N. Committee." Clin Neurophysiol **126**(6): 1071-1107.

Rotenberg, A., D. Depositario-Cabacar, E. H. Bae, C. Harini, A. Pascual-Leone and M. Takeoka (2008). "Transient suppression of seizures by repetitive transcranial magnetic stimulation in a case of Rasmussen's encephalitis." Epilepsy & Behavior **13**(1): 260-262.

Routley, B. C., K. D. Singh, K. Hamandi and S. D. Muthukumaraswamy (2017). "The effects of AMPA receptor blockade on resting magnetoencephalography recordings." Journal of Psychopharmacology **31**(12): 1527-1536.

Salavati, B., Z. J. Daskalakis, R. Zomorrodi, D. M. Blumberger, R. Chen, B. G. Pollock and T. K. Rajji (2018a). "Pharmacological Modulation of Long-Term Potentiation-Like Activity in the Dorsolateral Prefrontal Cortex." Frontiers in Human Neuroscience **12**(155).

Salavati, B., T. K. Rajji, R. Zomorrodi, D. M. Blumberger, R. Chen, B. G. Pollock and Z. J. Daskalakis (2018b). "Pharmacological Manipulation of Cortical Inhibition in the Dorsolateral Prefrontal Cortex." Neuropsychopharmacology **43**(2): 354-361.

Satlin, A., L. D. Kramer and A. Laurenza (2013). "Development of perampanel in epilepsy." Acta Neurologica Scandinavica **127**(s197): 3-8.

Schadel, M., D. Wu, S. V. Otton, W. Kalow and E. M. Sellers (1995). "Pharmacokinetics of Dextromethorphan and Metabolites in Humans: Influence of the CYP2D6 Phenotype and Quinidine Inhibition." Journal of Clinical Psychopharmacology **15**(4).

Schwenk, J., D. Baehrens, A. Haupt, W. Bildl, S. Boudkkazi, J. Roeper, B. Fakler and U. Schulte (2014). "Regional Diversity and Developmental Dynamics of the AMPA-Receptor Proteome in the Mammalian Brain." Neuron **84**(1): 41-54.

Seeck, M., L. Koessler, T. Bast, F. Leijten, C. Michel, C. Baumgartner, B. He and S. Beniczky (2017). "The standardized EEG electrode array of the IFCN." Clin Neurophysiol **128**(10): 2070-2077.

Shafi, M. M., M. Vernet, D. Klooster, C. J. Chu, K. Boric, M. E. Barnard, K. Romatoski, M. B. Westover, J. A. Christodoulou, J. D. E. Gabrieli, S. Whitfield-Gabrieli, A. Pascual-Leone and B. S. Chang (2015). "Physiological consequences of abnormal connectivity in a developmental epilepsy." Annals of Neurology **77**(3): 487-503.

Shin, E.-J., J.-H. Bach, S. Y. Lee, J. M. Kim, J. Lee, J.-S. Hong, T. Nabeshima and H.-C. Kim (2011). "Neuropsychotoxic and Neuroprotective Potentials of Dextromethorphan and Its Analogs." Journal of Pharmacological Sciences **116**(2): 137-148.

Shinnick-Gallagher, P., M. G. McKERNAN, J. XIE and F. ZINEBI (2003). "L-Type Voltage-Gated Calcium Channels Are Involved in the in Vivo and in Vitro Expression of Fear Conditioning." Annals of the New York Academy of Sciences **985**(1): 135-149.

Shitak, R., A. Sahai, D. Hota and A. Chakrabarti (2006). "Anti-seizure efficacy of nimodipine in pentylenetetrazole and kainic acid combined seizure models in mice." Indian journal of physiology and pharmacology **50**: 265-272.

Siebner, H. R. and U. Ziemann (2007). Das TMS-Buch: Handbuch der transkraniellen Magnetstimulation, Springer Berlin Heidelberg.

Sjöström, P. J. and S. B. Nelson (2002). "Spike timing, calcium signals and synaptic plasticity." Current Opinion in Neurobiology **12**(3): 305-314.

Smith, M. J., J. C. Keel, B. D. Greenberg, L. F. Adams, P. J. Schmidt, D. A. Rubinow and E. M. Wassermann (1999). "Menstrual cycle effects on cortical excitability." Neurology **53**(9): 2069-2072.

Sobolevsky, A. I., M. P. Rosconi and E. Gouaux (2009). "X-ray structure, symmetry and mechanism of an AMPA-subtype glutamate receptor." Nature **462**(7274): 745-756.

Storelli, F., A. Matthey, S. Lenglet, A. Thomas, J. Desmeules and Y. Daali (2018). "Impact of CYP2D6 Functional Allelic Variations on Phenoconversion and Drug-Drug Interactions." Clin Pharmacol Ther **104**(1): 148-157.

Sutor, B. and J. J. Hablitz (1989). "EPSPs in rat neocortical neurons in vitro. I. Electrophysiological evidence for two distinct EPSPs." J Neurophysiol **61**(3): 607-620.

Takahama, K., H. Fukushima, Y. Isohama, H. Kai and T. Miyata (1997). "Inhibition of glycine currents by dextromethorphan in neurones dissociated from the guinea-pig nucleus tractus solitarii." British Journal of Pharmacology **120**(4): 690-694.

Taylor, C. P., S. F. Traynelis, J. Siffert, L. E. Pope and R. R. Matsumoto (2016). "Pharmacology of dextromethorphan: Relevance to dextromethorphan/quinidine (Nuedexta®) clinical use." Pharmacol Ther **164**: 170-182.

Taylor, P. C. J., V. Walsh and M. Eimer (2008). "Combining TMS and EEG to study cognitive function and cortico–cortico interactions." Behavioural Brain Research **191**(2): 141-147.

Teleńczuk, B., S. N. Baker, R. Kempter and G. Curio (2015). "Correlates of a single cortical action potential in the epidural EEG." NeuroImage **109**: 357-367.

ter Braack, E. M., C. C. de Vos and M. J. van Putten (2015). "Masking the Auditory Evoked Potential in TMS-EEG: A Comparison of Various Methods." Brain Topogr **28**(3): 520-528.

Thielscher, A., A. Opitz and M. Windhoff (2011). "Impact of the gyral geometry on the electric field induced by transcranial magnetic stimulation." Neuroimage **54**(1): 234-243.

Thut, G., D. Veniero, V. Romei, C. Miniussi, P. Schyns and J. Gross (2011). "Rhythmic TMS Causes Local Entrainment of Natural Oscillatory Signatures." Current Biology **21**(14): 1176-1185.

Tomassoni, D., A. Lanari, G. Silvestrelli, E. Traini and F. Amenta (2008). "Nimodipine and its use in cerebrovascular disease: evidence from recent preclinical and controlled clinical studies." Clin Exp Hypertens **30**(8): 744-766.

Tortella, F. C., D. A. Martin, C. P. Allot, J. A. Steel, T. P. Blackburn, B. E. Loveday and N. J. Russell (1989). "Dextromethorphan attenuates post-ischemic

hypoperfusion following incomplete global ischemia in the anesthetized rat." Brain Res **482**(1): 179-183.

Traynelis, S. F., L. P. Wollmuth, C. J. McBain, F. S. Menniti, K. M. Vance, K. K. Ogden, K. B. Hansen, H. Yuan, S. J. Myers and R. Dingledine (2010). "Glutamate receptor ion channels: structure, regulation, and function." Pharmacol Rev **62**(3): 405-496.

Tremblay, S., N. C. Rogasch, I. Premoli, D. M. Blumberger, S. Casarotto, R. Chen, V. Di Lazzaro, F. Farzan, F. Ferrarelli, P. B. Fitzgerald, J. Hui, R. J. Ilmoniemi, V. K. Kimiskidis, D. Kugiumtzis, P. Lioumis, A. Pascual-Leone, M. C. Pellicciari, T. Rajji, G. Thut, R. Zomorrodi, U. Ziemann and Z. J. Daskalakis (2019). "Clinical utility and prospective of TMS-EEG." Clin Neurophysiol **130**(5): 802-844.

Tsai, J. J., T. Wu, H. Leung, T. Desudchit, S. Tiamkao, K. S. Lim and A. Dash (2018). "Perampanel, an AMPA receptor antagonist: From clinical research to practice in clinical settings." Acta Neurol Scand **137**(4): 378-391.

Tse, N. Y., M. R. Goldsworthy, M. C. Ridding, J. P. Coxon, P. B. Fitzgerald, A. Fornito and N. C. Rogasch (2018). "The effect of stimulation interval on plasticity following repeated blocks of intermittent theta burst stimulation." Scientific Reports **8**(1): 8526.

Turner, R. W., D. Anderson and G. W. Zamponi (2011). "Signaling complexes of voltage-gated calcium channels." Channels (Austin) **5**(5): 440-448.

Valentin, A., R. Arunachalam, A. Mesquita-Rodrigues, J. J. Garcia Seoane, M. P. Richardson, K. R. Mills and G. Alarcon (2008). "Late EEG responses triggered by transcranial magnetic stimulation (TMS) in the evaluation of focal epilepsy." Epilepsia **49**(3): 470-480.

Vandenberghe, W., W. Robberecht and J. R. Brorson (2000). "AMPA receptor calcium permeability, GluR2 expression, and selective motoneuron vulnerability." J Neurosci **20**(1): 123-132.

Veniero, D., M. Bortoletto and C. Miniussi (2009). "TMS-EEG co-registration: On TMS-induced artifact." Clinical Neurophysiology **120**(7): 1392-1399.

Verley, D. R., D. Torolira, B. Pulido, B. Gutman, A. Bragin, A. Mayer and N. G. Harris (2018). "Remote Changes in Cortical Excitability after Experimental Traumatic Brain Injury and Functional Reorganization." Journal of neurotrauma **35**(20): 2448-2461.

Voglis, G. and N. Tavernarakis (2006). "The role of synaptic ion channels in synaptic plasticity." EMBO reports **7**(11): 1104-1110.

Vyklicky, V., M. Korinek, T. Smejkalova, A. Balik, B. Krausova, M. Kaniakova, K. Lichnerova, J. Cerny, J. Krusek, I. Dittert, M. Horak and L. Vyklicky (2014). "Structure, function, and pharmacology of NMDA receptor channels." Physiol Res **63 Suppl 1**: S191-203.

Wankerl, K., D. Weise, R. Gentner, J. J. Rumpf and J. Classen (2010). "L-type voltage-gated Ca2+ channels: a single molecular switch for long-term potentiation/long-term depression-like plasticity and activity-dependent metaplasticity in humans." J Neurosci **30**(18): 6197-6204.

Wassermann, E. M. (1998). "Risk and safety of repetitive transcranial magnetic stimulation: report and suggested guidelines from the International Workshop on the Safety of Repetitive Transcranial Magnetic Stimulation, June 5–7, 1996." Electroencephalography and Clinical Neurophysiology/Evoked Potentials Section **108**(1): 1-16.

Weise, D., J. Mann, J. J. Rumpf, S. Hallermann and J. Classen (2017). "Differential Regulation of Human Paired Associative Stimulation-Induced and Theta-Burst Stimulation-Induced Plasticity by L-type and T-type Ca2+ Channels." Cereb Cortex **27**(8): 4010-4021.

Weisz, N., T. Hartmann, N. Müller and J. Obleser (2011). "Alpha Rhythms in Audition: Cognitive and Clinical Perspectives." Frontiers in Psychology **2**(73).

Werling, L. L., E. C. Lauterbach and U. Calef (2007). "Dextromethorphan as a potential neuroprotective agent with unique mechanisms of action." Neurologist **13**(5): 272-293.

Wolters, A., F. Sandbrink, A. Schlottmann, E. Kunesch, K. Stefan, L. G. Cohen, R. Benecke and J. Classen (2003). "A Temporally Asymmetric Hebbian Rule Governing Plasticity in the Human Motor Cortex." Journal of Neurophysiology **89**(5): 2339-2345.

Woodworth, J. R., S. R. Dennis, L. Moore and K. S. Rotenberg (1987). "The polymorphic metabolism of dextromethorphan." J Clin Pharmacol **27**(2): 139-143.

Xiang, J., K. Leiken, X. Degrauw, B. Kay, H. Fujiwara, D. F. Rose, J. R. Allen, J. E. Kacperski, H. L. O'Brien, M. A. Kabbouche, S. W. Powers and A. D. Hershey (2016). "Spatial Heterogeneity of Cortical Excitability in Migraine Revealed by Multifrequency Neuromagnetic Signals." The journal of pain : official journal of the American Pain Society **17**(6): 694-706.

Yu, A., H. Dong, D. Lang and R. L. Haining (2001). "Characterization of dextromethorphan O- and N-demethylation catalyzed by highly purified recombinant human CYP2D6." Drug Metab Dispos **29**(11): 1362-1365.

Ziemann, U. (2011). "Transcranial magnetic stimulation at the interface with other techniques: a powerful tool for studying the human cortex." Neuroscientist **17**(4): 368-381.

Ziemann, U., R. Chen, L. G. Cohen and M. Hallett (1998). "Dextromethorphan decreases the excitability of the human motor cortex." Neurology **51**(5): 1320.

Ziemann, U., J. Reis, P. Schwenkreis, M. Rosanova, A. Strafella, R. Badawy and F. Müller-Dahlhaus (2015). "TMS and drugs revisited 2014." Clin Neurophysiol **126**(10): 1847-1868.

Zipser, C. M., I. Premoli, P. Belardinelli, N. Castellanos, D. Rivolta, T. Heidegger, F. Müller-Dahlhaus and U. Ziemann (2018). "Cortical Excitability and Interhemispheric Connectivity in Early Relapsing-Remitting Multiple Sclerosis Studied With TMS-EEG." Frontiers in neuroscience **12**: 393-393.

Declaration of own contribution of this dissertation

Erklärung zum Eigenanteil der Dissertationsschrift

Die Arbeit wurde im Fachbereich Medizin in der Eberhard-Karls-Universität zu Tübingen unter Betreuung von Herrn Prof. Dr. med. Ulf Ziemann durchgeführt.
Die Konzeption der Studie und Beantragung der Studienzulassung durch die Ethikkommission erfolgte in Zusammenarbeit von mir mit Herrn Prof. Dr. med. Ziemann, Herrn Dr. med. Florian Müller-Dahlhaus und Herrn Dr. med. Carl Zipser.
Die Versuche wurden durch mich und Frau Franca König in Zusammenarbeit mit gleichen Arbeitsanteilen durchgeführt. Die Festlegung des Promotionsthemas erfolgte nach Einverständnis des Promotionsausschusses der Eberhard-Karls-Universität zu Tübingen.
Meine Einarbeitung erfolgte durch Frau Dr. med. Julia Kiraly und Herrn Dr. med. Carl Zipser, der ebenfalls als Studienarzt fungierte.
Die statistische Auswertung und Bewertung erfolgten nach Anleitung durch Frau Dr. Debora Desideri und Herrn Dr. Paolo Belardinelli.
Ich versichere, das Manuskript selbständig verfasst zu haben und keine weiteren als die von mir angegebenen Quellen verwendet zu haben.

Tübingen, den 12.03.2021

Chen Liang

Danksagung

Diese Dissertation wurde mit tatkräftiger Unterstützung vieler Personen angefertigt, welchen ich im Folgenden danken möchte:
In erster Linie möchte ich mich bei meinem Doktorvater Prof. Ziemann für die Konzeption und das Anfertigen dieser experimentellen Promotionsarbeit bedanken, welche erst durch das Ermöglichen der Teilnahme an den äußerst interessanten Forschungsfortbildungen und die Unterstützung in der Orientierung und Deutung mit seinem unschätzbaren Wissen erfolgen konnte.
Meinem Betreuer Dr. Carl Zipser verdanke ich seine langjährige Hilfe und Mentoring, sowohl als Ratgeber, als auch als praktischer Anleiter und Studienarzt. Erst durch seine Begleitung in meiner akademischen Laufbahn konnte die vorliegende Dissertationsschrift vervollständigt werden.
Mein Dank gebührt ebenfalls Dr. Debora Desideri und Dr. Paolo Belardinelli, die mich durch die komplexen Sachverhalte der technischen und statistischen Auswertungen geführt haben und mit Ratschlägen meine Promotionsschrift tatkräftig unterstützt haben.
Zusätzlich bedanke ich mich bei Dr. Florian Müller-Dahlhaus für seine langjährige Unterstützung und Begleitung im Studienverlauf und für die Konzeption und Ethikbeantragung des Promotionsthemas.
Dr. Julia Kiraly verdanke ich herzlich die technischen Einweisungen und die Einführung in die Thematik.
Besonderen Dank gilt Frau Franca König für die gute Zusammenarbeit bei der gemeinsamen Durchführung unserer Experimente und Datenverarbeitung.
Nicht zuletzt möchte ich mich meiner Familie für die tägliche Unterstützung in meinem Promotionsvorhaben bedanken.